This manuscript, entitled ***Late Tonian development and provenance of the Adelaide Superbasin****,* is a preprint that has not undergone peer-review. It is a version of the manuscript is included within the PhD thesis this work forms part of. It is subject to further revision by co-authors prior to journal submission, reviews by thesis examiners, and the peer review process once submitted to a journal. If accepted once submitted to a journal, the final version of this manuscript will be available via the "published version" link at the top of this webpage. Please feel free to contact the main author; we welcome feedback and queries

Jarred C. Lloyd[1,2]; Alan S. Collins[1]; Morgan L. Blades[1]; Sarah E. Gilbert[3]; Kathryn J. Amos[2]

1. Tectonics and Earth Systems Group, and Mineral Exploration CRC, Department of Earth Sciences, University of Adelaide, Adelaide, SA 5005, Australia
2. Australian School of Petroleum and Energy Resources, University of Adelaide, Adelaide, SA 5005, Australia
3. Adelaide Microscopy, University of Adelaide, Adelaide, SA 5005, Australia

Corresponding author email: jarred.lloyd@adelaide.edu.au

Late Tonian development and provenance of the Adelaide Superbasin

Jarred C. Lloyd[1,2]; Alan S. Collins[1]; Morgan L. Blades[1]; Sarah E. Gilbert[3]; Kathryn J. Amos[2]

1. Tectonics and Earth Systems Group, and Mineral Exploration CRC, Department of Earth Sciences, University of Adelaide, Adelaide, SA 5005, Australia
2. Australian School of Petroleum and Energy Resources, University of Adelaide, Adelaide, SA 5005, Australia
3. Adelaide Microscopy, University of Adelaide, Adelaide, SA 5005, Australia

Abstract

The late Tonian sequences of the Adelaide Superbasin were witness to the birth of the proto-Pacific Ocean during the breakup of Rodinia. Understanding the sedimentology and provenance of these rocks from across the basin is key to understanding both their deposition over ~70 million years, the local palaeogeography, and leads to a better understanding of the early development of the proto-Pacific Ocean. While the sedimentology of the Burra Group is well studied in most areas, provenance studies on these sequences using detrital zircon have been limited in scope and lack both spatial and temporal diversity. In this study we begin to address this knowledge gap. Samples were taken from across the Adelaide Superbasin to understand both spatial and temporal related changes in provenance. Our findings highlight the necessity of this approach by uncovering both subtle, and abrupt significant changes in detrital zircon spectra for coeval samples from across the basin, and up-sequence in local areas. Our results highlight significant changes in provenance c. 790 Ma in the north of the basin, and c. 740 Ma in the south of the basin. This suggests a southward propagation of the rift basin, gradually opening to southerly sediment supply. Additionally, we posit the existence of an unrecognised source of c. 1000–900 Ma zircon to the north or northeast of the basin to account for latest Stenian to earliest Tonian detrital zircon in the Myrtle Springs Formation.

1 Introduction

The mid to late Tonian was a critical time in Earth's history, the breakup of the supercontinent Rodinia was well underway (Li et al. 2008; Merdith et al. 2017), numerous large igneous provinces were emplaced (Ernst et al. 2008), and the climate began to show hints of the oncoming pan-global glaciations of the Cryogenian (MacLennan et al. 2020). The record of this time is preserved in the many Tonian palaeo-rift sequences globally (Merdith et al. 2019). One of the most completely preserved successions laid down in the Tonian is that of the Adelaide Superbasin (Lloyd et al. 2020) in South Australia [Figure 1, Figure 2]. The primary rift sequences in the basin, the Callanna and Burra Groups, are key to understanding the evolution of the rift system and the basin's position within Rodinia. Compressive tectonic stresses (Foden et al. 2006; Foden et al. 2020; Hall 2018; Lubiniecki et al. 2020; Mackay 2011) have folded, uplifted and dismembered the sequences of the basin, and salt tectonics has significantly influenced the later depositional sequences of the basin (Heysen Supergroup, Moralana Supergroup) and disrupted many of the early rift sequences in the process (Counts et al. 2019; Mackay 2011; Mount 1976; Rowan et al. 2019). These factors, along with the vast size of the basin and the hundreds of millions of years since deposition, have made it difficult to understand the nuanced evolution of the basin as a whole. Numerous studies over many years have made great advances on understanding the evolution of the basin through time (e.g., Armistead et al. 2020; Betts et al. 2018; Counts & Amos 2016; Howchin 1904; Jago et al. 2018; Keeman et al. 2020; Lechte & Wallace 2015; Lloyd et al. 2020; Mackay 2011; Mancktelow 1979; Mawson 1947; Mawson & Sprigg 1950; Mount 1976; Murrell 1977; Preiss 1987; 2000; Rose et al. 2013; Sprigg 1952; Stüeken et al. 2019; Toteff 1977; Uppil 1980; Virgo et al. 2021; Williams, GE et al. 2008). However, detrital provenance studies, until recently (Keeman et al. 2020; Lloyd et al. 2020), had been small scale (Ireland et al. 1998; Job 2011; Shahin 2016), or specifically targeted (Rose et al. 2013). Detrital zircon studies provide supplementary, but particularly useful insight into the palaeo-tectonic/geographic evolution of a basin through time by investigating the change in source of robust detrital material. To date, limited, or very targeted detrital zircon data exists (Keeman et al. 2020; Lloyd et al. 2020; van der Wolff 2020) for the Burra Group, with key sequences (e.g., Myrtle Springs Formation) having no data. This has hindered attempts to understand the late Tonian evolution of the Adelaide Superbasin, and its place within Rodinia. Here we present detrital zircons from the Burra Group [Figure 3], with additional but limited data presented from the Yerelina Subgroup (representing the *Marinoan glaciation*) and Pound Subgroup (the uppermost sequences of the Adelaide Rift Complex). Due to the extensive literature available (e.g., Counts & Amos 2016; Counts et al. 2016; Le Heron 2012; Le Heron et al. 2011; Lloyd et al. 2020; Preiss 1993; 2000; Rose et al. 2013; Williams, GE et al. 2008) on the Yerelina and Pound Subgroups, and limited detrital zircon data presented for those subgroups in this study, we primarily focus on the provenance and evolution of the Burra Group. Notably, this study presents the first detrital zircon data that compares upper Emeroo Subgroup time equivalent sequences across the North Flinders Ranges (east-west) and additionally lays the framework for better understanding the north-south evolution of the basin during deposition of the Burra Group.

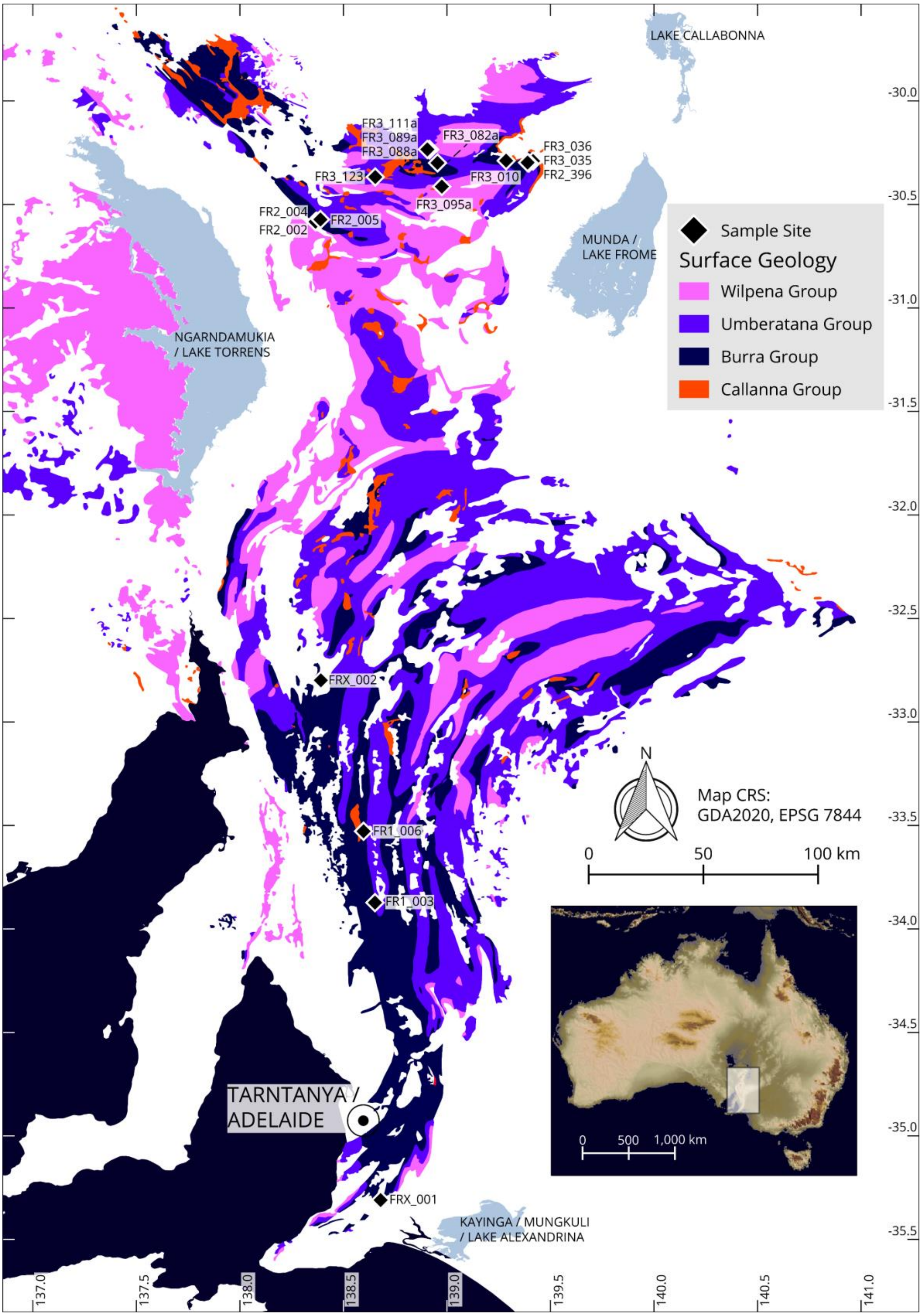

Figure 1 – Map showing surface geology distribution of the Neoproterozoic sequences of the Adelaide Rift Complex, Stuart Shelf, and Coombalarnie Platform. Sample sites from this study are indicated by diamonds. For GPS coordinates of the sample sites see data availability. Inset map shows location of main map relative to the Australian landmass as colour shade map overlain on hill shaded GMTED2010 7.5s digital elevation model, publicly available from the United States Geological Survey (Danielson & Gesch 2011).

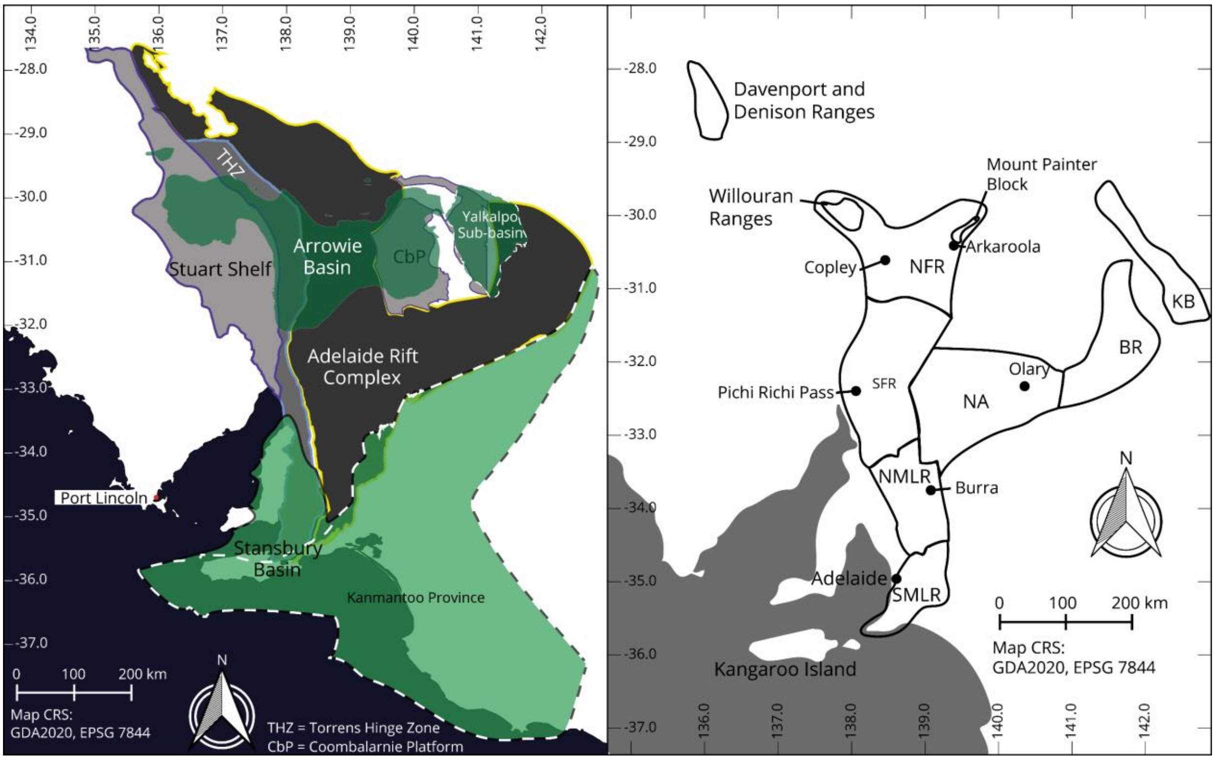

Figure 2 – Left: Subdivisions of the Adelaide Superbasin. Greys are the Neoproterozoic basins; greens are the Cambrian basins. Right: Geographic divisions of the Adelaide Superbasin referred to in text. Abbreviations: MLR-Mount Lofty Ranges, FR-Flinders Ranges (N=North, S=South); NA-Nackara Arc; BR-Barrier Ranges; KB-Koonenberry Belt

2 Geological Background

2.1 Adelaide Superbasin

The Adelaide Superbasin (Lloyd et al. 2020) is a large, Neoproterozoic to middle Cambrian sedimentary system at the southeast margin of Proterozoic Australia, which formed as a result of the breakup of the supercontinent Rodinia. The Adelaide Superbasin consists of several named basins and sub-basins [Figure 2] that span the Neoproterozoic to early Cambrian (Lloyd et al. 2020). The largest and oldest of these is the Adelaide Rift Complex, which is contiguous with the relatively undeformed rocks of the Torrens Hinge Zone, Stuart Shelf (Sprigg 1952), and Coombalarnie Platform (Callen 1990). Two Cambrian basins, the Arrowie Basin, and the Stansbury Basin, are also considered as part of the Adelaide Superbasin (Lloyd et al. 2020; Preiss et al. 2002). Deposition within the Adelaide Superbasin spans over 300 million years of Earth's history and stretches from the northernmost regions of South Australia, narrowing in the South Mount Lofty Ranges at the Fleurieu Peninsula and extending onto Kangaroo Island. The basin began as an intracontinental rift system that successfully progressed to a passive margin basin in its southeast region, yet remained a failed rift in the north (Lloyd et al. 2022b, preprint). Deposition within the basin ceased during the Delamerian orogeny c. 514–490 Ma (Drexel & Preiss 1995; Foden et al. 2006; Foden et al. 2020; Preiss 2000). Whilst present day exposure of the sedimentary basin is approximately 600 km north to south, the basin spans over 1,100 km from central Australia through to

Kangaroo Island. The stratigraphy of the Adelaide Superbasin is divided into three supergroups (Lloyd et al. 2020; Preiss 2000), two for the Neoproterozoic sequences and the third for the Cambrian sequences, with numerous group and subgroup level divisions. In the Neoproterozoic, the Warrina Supergroup is comprised of the Callanna, Burra, and Poolamacca Groups, and the Heysen Supergroup contains the Umberatana, Wilpena, Torrowangee, and Farnell Groups. Each of these groups are further divided into numerous subgroups. The reader is referred to Preiss (1987), Preiss (2000), Counts (2017), Lloyd et al. (2020), Cowley (2020) and references therein for further detail on the geological history of the Adelaide Superbasin.

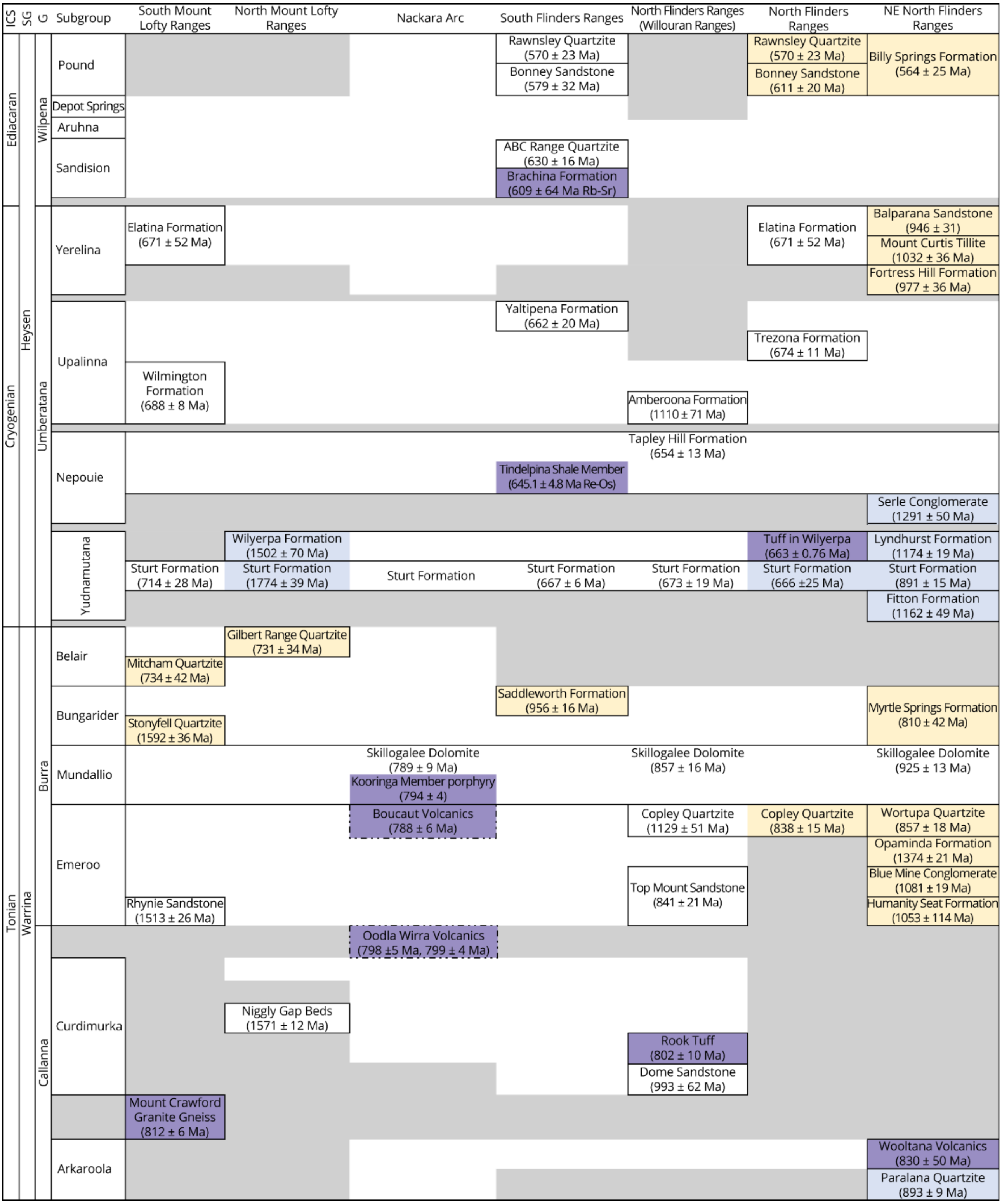

Figure 3 – Stratigraphic table showing supergroup (SG), group (G), and subgroup divisions of the Neoproterozoic successions of the Adelaide Superbasin. Formations with available geochronology are shown accordingto their geographic locality (headers). Yellow shading indicates formations detrital constraints new from this study, or where new data has been added to existing data from Keeman et al. (2020) and Lloyd et al. (2020), mauve shading indicates data from (Lloyd et al. 2022d, preprint), white shading indicates detrital data from Keeman et al. (2020) and Lloyd et al. (2020), and purple shading indicates non-detrital chronology. Adapted from Lloyd et al. (2020).

2.1.1 Burra Group

The Burra Group is the first widely preserved and exposed series of rocks in the Adelaide Rift Complex of the Adelaide Superbasin. The group is comprised of a generally thick sequence of siliciclastic and carbonate rocks [Figure 4] and is divided into four subgroups (Preiss 1987; 2000; Preiss & Cowley 1999). It is known to unconformably overlay the Callanna Group near the margins of the basin but the true stratigraphic contact between the two groups in areas of a more complete sequence of Callanna Group is not known (Preiss 1987). Circumstantial evidence has been used to infer a regional unconformity (e.g., Murrell 1977). The Burra Group unconformably overlies basement in the southern area of the basin (South Mount Lofty Ranges). It is unconformably overlain by the Umberatana Group, with the termination of the Burra Group occurring at the boundary between the Tonian and Cryogenian periods, marking the start of the *Sturtian glaciation* in South Australia. The basal Emeroo Subgroup is the oldest subdivision and is made of primarily arenaceous rocks with minor dolomitic rocks and mafic volcanics [Figure 4]. The base of the Burra Group is defined as the first influx of coarse clastic material after the Curdimurka Subgroup of the Callanna Group (Preiss 1993). In the south of the basin the Emeroo Subgroup remains as coarse clastic rocks, but in all other areas it transitions to finer clastic and carbonate sequences before transitioning back to coarser clastic rocks. The top of the Emeroo Subgroup is marked by a widespread series of laterally correlative quartzites/sandstones (e.g., Copley Quartzite, Wortupa Quartzite) that conformably transition into the primarily dolomitic sequences of the Mundallio Subgroup (e.g., Skillogalee Dolomite, Montacute Dolomite). Minor volcanism is known to occur within the Skillogalee Dolomite c. 790 Ma and is believed to be responsible for mineralisation (Preiss et al. 2009) at the closed Burra Copper Mine, which produced ~2.7 million tonnes of copper ore during its lifetime (Drexel 2008). A significant amount of variation is present within the lithologies of the Skillogalee Dolomite and its equivalents, but sedimentary magnesite and abundant dolostones characterise this subgroup (Counts 2017; Preiss 1987; 2000; Uppil 1980; Virgo et al. 2021). Geochronology supports correlation of the Boucaut Volcanics to the volcanics occurring within the Skillogalee Dolomite c. 790 Ma (Armistead et al. 2020; Preiss et al. 2009). After deposition of the mostly paralic sedimentary sequences of the Mundallio Subgroup, the conformably overlying Bungarider Subgroup sees a return to increasingly clastic deposition (Counts 2017; Preiss 2000; Virgo et al. 2021), with subsequent sourceward-shifting to basinward-shifting facies tracts [Figure 4]. Only present in the south and east of the basin, the Belair Subgroup is still poorly understood, but shows greater lithological similarity to the underlying Bungarider Subgroup than it does to the overlying Umberatana Group (Counts 2017). At its base, the Belair Subgroup consists of coarse grained quartzites, with an overall sourceward-shifting facies tract to the upper, predominantly shale sequences [Figure 4]. Very rare lonestones in the uppermost Mintaro Shale allow for the possibly of minor shore ice (Preiss 2000).

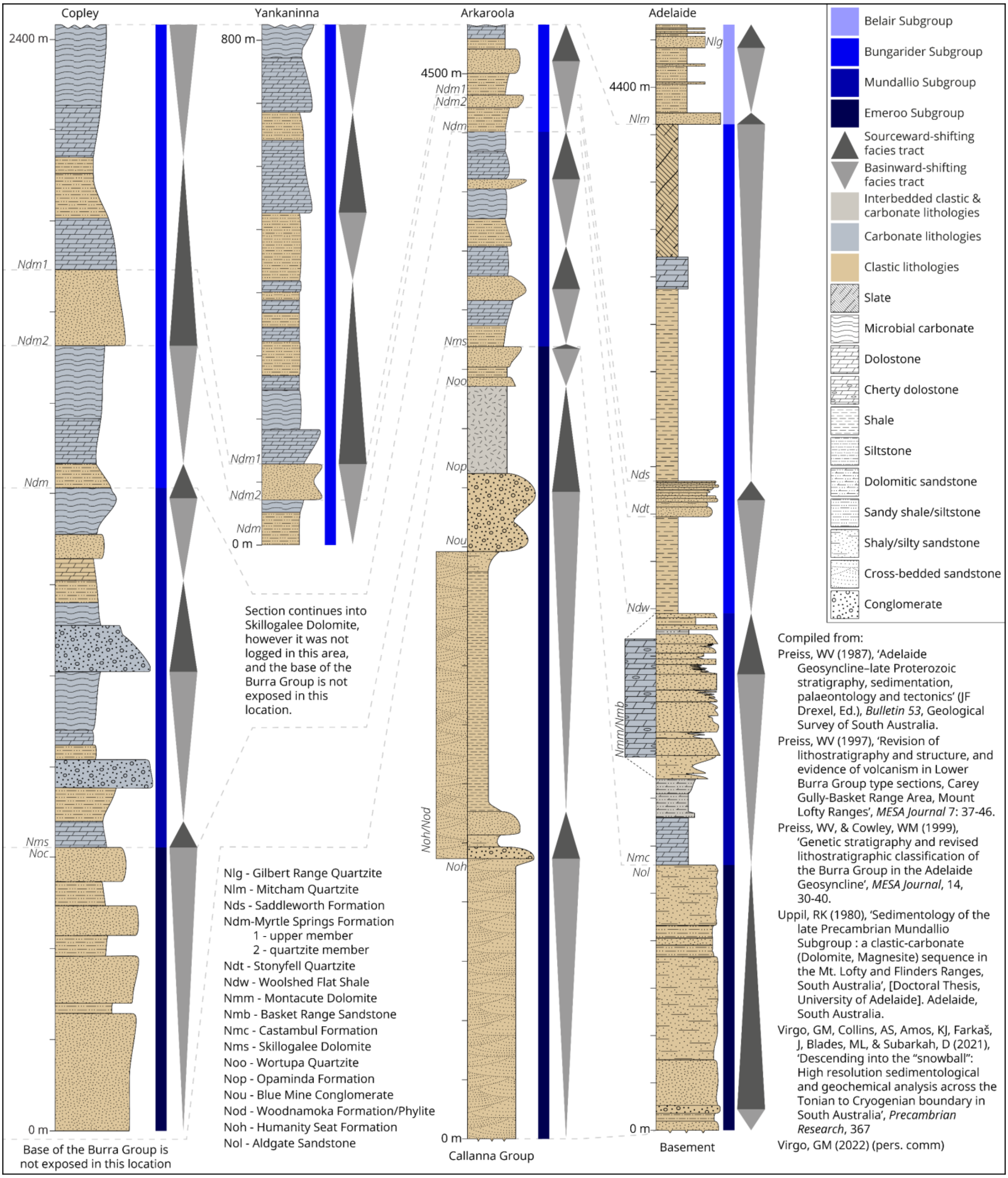

Figure 4 – Generalised stratigraphic columns with correlation lines of the Burra Group from the south and north of the basin with corresponding, high level, tectonic sequence stratigraphy facies. Tectonic successions follow terminology of Matenco and Haq (2020), sourceward-shifting facies tracts are where accommodation space is created faster than the rate of sediment supply (δAS/SS = >1) and basinward-shifting facies tracts are where the rate of sediment supply outdoes the creation of accommodation space (δAS/SS = <1). Stratigraphic logs compiled from Preiss (1987; 1997); Preiss and Cowley (1999); Uppil (1980); Virgo et al. (2021), and GM Virgo (pers. comm). For location references, refer to the map figures.

2.1.2 Umberatana Group

The Umberatana Group disconformably overlies the Burra Group, and is further divided into the Yudnamutana, Nepouie, and Yerelina Subgroups. The Yudnamutana Subgroup is made up of glaciogenic rocks attributed to the *Sturtian glaciation*, dominated by globally significant, characteristic diamictites of the Sturt Formation (Lloyd et al. 2022d, preprint). The overlying Nepouie subgroup marks the first basin-wide flooding event, signified by the ubiquitous Tapley Hill Formation (Preiss 1987; 1993; 2000). Further detail on the stratigraphy of Yudnamutana and Nepouie Subgroups is found in Preiss (1987; 2000) and Lloyd et al. (2022d, preprint). The Yerelina Subgroup overlies the Nepouie Subgroup and is detailed further here.

2.1.2.1 Yerelina Subgroup

The Yerelina Subgroup is the uppermost division of the Umberatana Group and represents the *Marinoan (Elatina) glaciation* in South Australia. The equivalent subgroup in New South Wales is thought to be the Teamsters Creek Subgroup (Cooper & Tuckwell 1971; Fitzherbert & Downes 2015; Preiss 1987; Sheibner & Basden 1998). In the far north-eastern (North Flinders Ranges) and southeast to east of the basin (North Mount Lofty Ranges, Nackara Arc), the Fortress Hill Formation is the lowermost formation in the subgroup and represents the onset of glacial conditions, marked by the presence of small drop stones and occasional boulders within laminated siltstones (Lindsay 1973; Preiss et al. 1998). The abundance of clasts increases toward the top of the formation, and the presence of crossbedding and sinuous ripple marks are suggested to indicate overall shallowing of the formation (Lindsay 1973). Overlying the Fortress Hill Formation is the Mount Curtis Tillite, and Gumbowie Arkose. Along with the Pepuarta Tillite (conformably overlies the Gumbowie Arkose), the Mount Curtis Tillite is believed to represent the glacial maximum during this time. These units are thought to be deposited under high-energy, shallow-water conditions (Preiss et al. 1998) with clear glacial origin indicated by faceted and striated boulders within the diamictites (Williams, GE et al. 2011). These in turn are overlain by the deglacial Balparana Sandstone, Grampus Quartzite and Ketchowla Siltstone. In the far south (Adelaide area), central (South and North Flinders Ranges) and west (Stuart Shelf) of the basin, the Elatina Formation and Whyalla Sandstone are the correlatives of the aforementioned units, with the exception of the Fortress Hill Formation. The Elatina Formation is much thinner at its maximum, attaining up to ~300 m in thickness (Rose et al. 2013), compared to the correlative Mount Curtis Tillite and Balparana Sandstone ~1000 m (Preiss 1993). The Elatina Formation contains significant variation in lithology from glaciofluvial to deltaic and shallow marine sandstones, glaciomarine diamictites, siltstones and mudstones with ice-rafted drop stones, and tidal rhythmites (Le Heron 2012; Le Heron et al. 2011; Preiss 1993; 2000; Rose et al. 2013; Williams, GE et al. 2008). The Whyalla Sandstone as currently defined contains a characteristic peri-glacial aeolian sandstone (Williams, GE et al. 2008; Williams, GE & Tonkin 1985) with fluvial to deltaic and marine variations (McAvaney et al. 2016; Tonkin & Wallace 2021). The Yerelina Subgroup is overlain by a distinct cap carbonate in almost all areas, marking the end of the *Marinoan (Elatina) glaciation.* This cap carbonate is globally ubiquitous and dated at c. 635 Ma (Calver et al. 2013; Rooney et al. 2015).

2.1.3 Wilpena Group

The Wilpena Group is the uppermost division of the Neoproterozoic sequences of the Adelaide Superbasin and is broadly divided in to two broad, upward shoaling sequences. The first of these corresponds to the Sandison Subgroup, which is the lowermost stratigraphic subdivision of the Wilpena Group. This subgroup begins with the Nuccaleena Formation (the cap carbonate of the *Marinoan glaciation*) which is generally overlain by, but partially coeval to the Seacliff Sandstone. These units are in turn overlain by the Brachina Formation and its equivalents, predominantly shales and siltstones that shallow upward into the ABC Range Quartzite (Counts 2017; Preiss 1987; 2000). As currently defined, the Aruhna Subgroup (Bunyeroo Formation and equivalent Yarloo Shale) overlies the Sandison Subgroup, and is then overlain by the Depot Springs Subgroup (Wonoka Formation, Wearing Dolomite). The Aruhna and Depot Springs Subgroup divisions remain conjectural and are likely unwarranted (Preiss 2000). The Bunyeroo Formation and Yarloo Shale are thought to have been deposited under a cold-water, generally deep-marine setting in an overall transgressive sequence (Young 1995). Notably, the Bunyeroo Formation and Yarloo Shale contain a distinct layer interpreted as a bolide impact debris layer related to an impact site at Lake Acraman (Gostin et al. 1986). The Wonoka Formation has been subject to numerous studies (e.g., Eickhoff et al. 1988; Giddings et al. 2010; Haines 1987; Retallack et al. 2014; Urlwin 1992) owing to the presence of deeply incised canyons and a strongly negative $\delta^{13}C$ anomaly known as the Shuram-Wonoka excursion (Williams, GE & Schmidt 2018). The overlying Pound Subgroup is the uppermost division of the Wilpena Group, and the last of the Neoproterozoic sequences in the Adelaide Superbasin. It contains three formations, the basal Bonney Sandstone and the Rawnsley Quartzite (Counts 2017). Both formations are replaced by the Billy Springs Formation in the far northeast Flinders Ranges (Counts & Amos 2016; Sheard 2012). The Bonney Sandstone primarily consists of fine to medium grained, reddish quartz arenites to feldspathic sandstones but is occasionally coarse grained. It is interpreted to have been deposited in a tidally influenced marginal marine environments, with some support for a tidal-estuary system (Gehling 1983; Preiss 1987). However, a more recent study in the type area did not determine conclusive evidence for tidal influence, instead suggesting a fluvially dominated deltaic sequence, with only a small contribution from waves and tides (Counts et al. 2016). Both studies concur that Bonney Sandstone is a shallowing upward sequence. One formal member is defined for the Bonney Sandstone, the carbonate rich Patsy Hill Member (Preiss 1999). The Bonney Sandstone disconformably underlies the Chace Quartzite Member of the Rawnsley Quartzite, whilst also being incised by the Ediacara Member locally (Gehling & Droser 2012). Overall, the Rawnsley Quartzite is made up of cleaner sandstones than those of the Bonney Sandstone and is thought to be deposited as a shallow marine, wave and tide reworked deltaic succession (Gehling 2000; Gehling & Droser 2012). The Rawnsley Quartzite is most famous for the Ediacara Member that preserves fossil casts of the Ediacaran fauna (Gehling & Droser 2012), Earth’s first confirmed animals (Bobrovskiy et al. 2018).

3 Methods

Methodology is that of Lloyd et al. (2022b, preprint) with a summary provided here.

Rock samples were prepared for detrital zircon analysis by crushing, sieving, panning and, where necessary due to low zircon yield, heavy liquid separation. Any grain that remotely resembled a zircon was picked to minimise human bias, an issue highlighted by Sláma and Košler (2012) and Dröllner et al. (2021). Where permitted by zircon yields, at least 300 zircons were picked per sample, otherwise all zircons in the sample were picked. Cathodoluminescence images were obtained on either a FEI Quanta 600 scanning electron microscope (for zircon analysed in 2020) or a Cameca SXFive Electron Microprobe (for zircon analysed in 2021). The zircons were using Laser Ablation Inductively Coupled Plasma Mass Spectrometry (LA-ICP-MS) to obtain a suite of elemental data for U–Pb geochronology and rare earth element (REE) analysis. All zircons were analysed using a Resonetics M-50 (193 nm ArF excimer) laser ablation system coupled with an Agilent 7900x inductively coupled plasma mass spectrometer. All analytical instruments used are housed at Adelaide Microscopy, University of Adelaide, Australia.

GJ-1 (Horstwood et al. 2016; Jackson et al. 2004), was used as the primary calibration standard for U–Pb ratios and NIST610 (Jochum et al. 2011) was used as the primary calibration standard for Pb isotope ratios and trace element data. The internal standard for trace element data was set to ^{91}Zr with a value of 431,400 ppm (43.14 wt%) assigned to unknowns. Plešovice (Horstwood et al. 2016; Sláma et al. 2008) and 91500 (Horstwood et al. 2016; Wiedenbeck et al. 1995; Wiedenbeck et al. 2004) were used as validation standards. Unknowns were bracketed by two analyses of GJ-1, followed by a combined two to three analyses of Plešovice and 91500, and two analyses of NIST610 every 20–30 unknowns. A 30 second gas blank followed by either a 40 second or 30 second ablation (session on 2021-03-30) time was used with a laser repetition rate of 5 Hz. A spot size of 29 µm and a nominal fluence of 2 Jcm^{-2} was used for zircon, and a spot size of 43 µm using a nominal fluence of 3.5 Jcm^{-2} was used for NIST610. Data were processed using LADR (Norris & Danyushevsky 2018), version 1.1.06 and output as “Full Analytical Uncertainty”. No common Pb corrections were applied to the data. Reference material ratios for GJ-1, Plešovice, and 91500 were set to the Chemical Abrasion Isotope Dilution Thermal Ionisation Mass Spectrometry (CA-ID-TIMS) values (uncorrected for thorium disequilibria and common-Pb) of Horstwood et al. (2016). Weighted averages and dispersion statistics for all standards are available from the link in data availability.

Statistical analysis of the zircon U–Pb data follows the method of Lloyd et al. (2020). Data are considered concordant if within ± 10%, and a “meaningful” age if the 2σ uncertainty is ≤10%—if a datum satisfies both parameters it is termed a *Filtered Age*. Maximum depositional ages are determined from a stricter 2% concordance filter and use the older age of the three isotope ratios (^{207}Pb/^{235}U, ^{206}Pb/^{238}U, ^{207}Pb/^{206}Pb) for a conservative estimate of the youngest single concordant grain. All ages are quoted with 2σ uncertainty. Kernel density estimates (KDEs), and multidimensional scaling plots

(MDS) were generated using IsoplotR (Vermeesch 2018). Key zircon trace element data are presented graphically using methods following Verdel et al. (2021) and additionally lanthanoid data are represented using violin plots and lambda representation (Anenburg 2020; O'Neill 2016).

Metadata for the LA-ICP-MS sessions, data for all analyses, cathodoluminescence images, and R code used to generate plots are available from the links in data and code availability.

4 Results

Fifteen samples from the Burra Group (FR1_003_01, FR1_006_03, FR2_002_01, FR2_004_01, FR2_005_01, FR2_396, FR3_010, FR3_035, FR3_036, FR3_082a, FR3_123, FRX_001, FRX_002, ML_008, & SF1), three samples from the Umberatana Group (FR3_088a, FR3_089a, & FR3_111a), and three samples from the Wilpena Group (058, 319, & FR3_095a) were analysed for detrital zircon geochronology and provenance. Several samples had naturally low zircon yields (FR1_006_03, FR3_035. FR3_036, FR3_088a, FR3_089a, FR3_111a, & FRX_001). Additional zircon analyses on samples 058 and 319 from Lloyd et al. (2020) were run during this study. The youngest grains quoted here for the Minburra Quartzite Member and Billy Springs Formation are too young to be reliable ages, particularly as maximum depositional ages, this is attributed to be an artefact of concordance determination outlined in the methods section, and mostly likely a result of minor Pb-loss post crystallisation. This highlights the need to use a conservative and strict method for determining maximum depositional ages when using youngest single grains, as is outlined in the method section by using a stricter 2% concordance filter, and the oldest of the three derived ages for a grain.

4.1 Burra Group

A total of 89 zircons were analysed from sample FR2_396, Opaminda Formation, with 66 passing filtering parameters. Grain ages range from 3164 ± 32 Ma to 1117 ± 17 Ma, with a primary population peak c. 1590 Ma. Subordinate population peaks are present c. 3130 Ma, c. 2640 Ma, c. 2480 Ma, c. 1760 Ma and c. 1410 Ma [Figure 5].

A total of 28 zircons were analysed from sample FR3_036, Humanity Seat Formation, with 26 passing filtering parameters. Grain ages range from 2535 ± 32 Ma to 1017 ± 18 Ma, with a primary population peak c. 1640 Ma, and a secondary population peak c. 2480 Ma [Figure 5].

A total of 40 zircons were analysed from sample FR3_035, Blue Mine Conglomerate, with 38 passing filtering parameters. Grain ages range from 2978 ± 32 Ma to 1079 ± 17 Ma, with a primary population peak c. 1710 Ma, and a secondary population peak c. 2480 Ma [Figure 5].

A total of 56 zircons were analysed from sample FR3_010, Wortupa Quartzite, with 56 passing filtering parameters. Grain ages range from 3239 ± 59 Ma to 845 ± 13 Ma, with a primary population peak c. 1720–1640 Ma, and a subordinate population peaks c. 3120 Ma, c. 2400 Ma, and c. 1000 Ma [Figure 5].

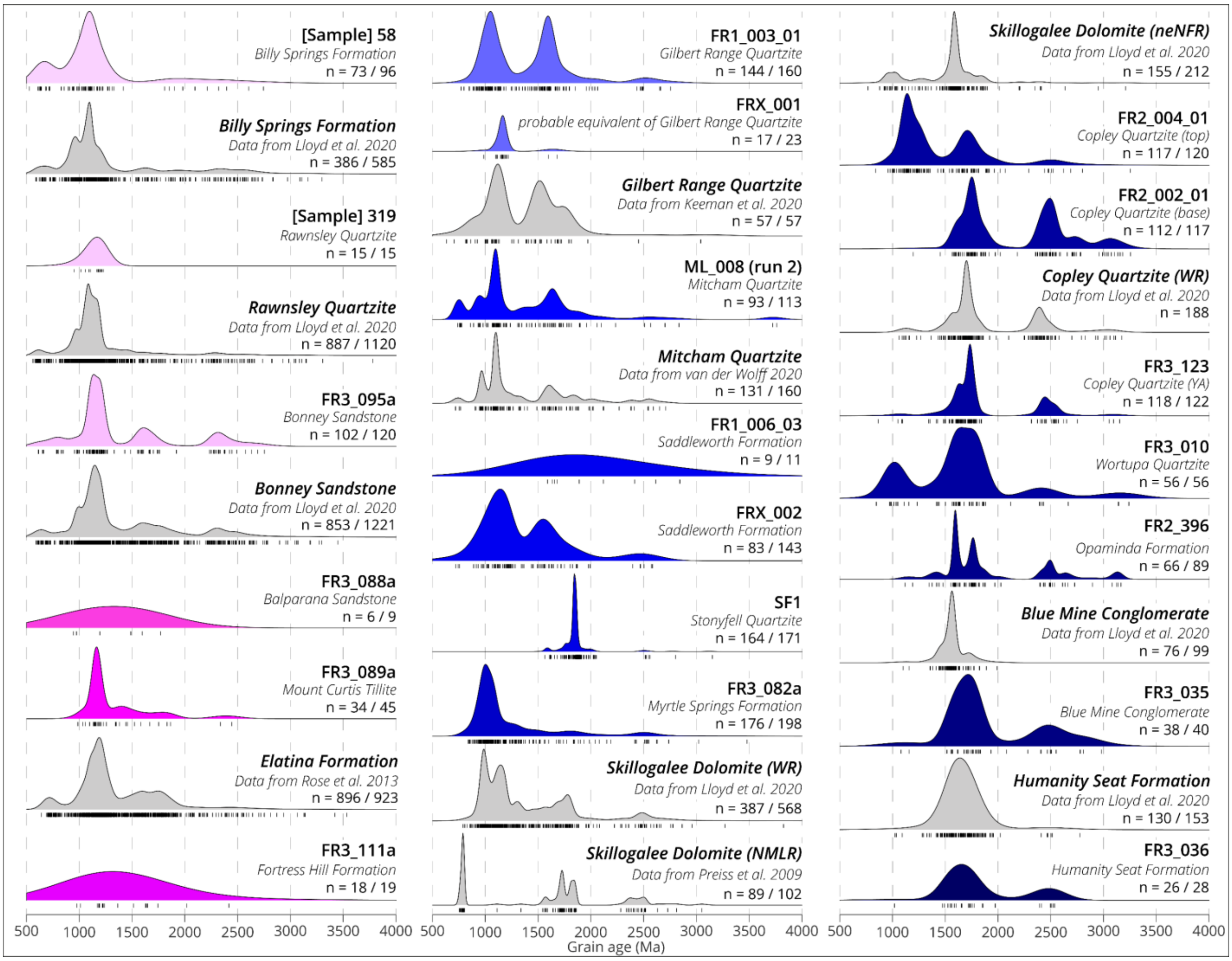

Figure 5 – Kernel density estimates [KDEs] of detrital zircon populations from each sample. Coloured KDEs are from data collect in this study, while grey KDEs are from published sources as denoted. Tick marks below each plot represent an analysis. n = filtered analyses / total analyses. Generated using IsoplotR (Vermeesch 2018). Abbreviations: WR = Willouran Ranges; neNFR = north-eastern North Flinders Ranges; YA = Yankaninna area/anticline; NMLR = North Mount Lofty Ranges

A total of 122 zircons were analysed from sample FR3_123, Copley Quartzite (Yankaninna area), with 118 passing filtering parameters. Grain ages range from 3152 ± 27 Ma to 864 ± 16 Ma with a primary population peak c. 1720 Ma, and a subordinate population peaks c. 2430 Ma, and c. 1620 Ma [Figure 5].

A total of 117 zircons were analysed from sample FR2_002_01, Copley Quartzite (Copley area, base), with 112 passing filtering parameters. Grain ages range from 3254 ± 36 Ma to 1195 ± 20 Ma, with a primary population peak c. 1750 Ma. Subordinate population peaks are present at c. 3050 Ma, c. 2720 Ma, and c. 2480 Ma [Figure 5].

A total of 120 zircons were analysed from sample FR2_004_01, Copley Quartzite

(Copley area, top), with 117 passing filtering parameters. Grain ages range from 3252 ± 33 Ma to 838 ± 13 Ma, with a primary population peak c. 1130 Ma. Subordinate population peaks are present c. 2490 Ma, and c. 1690 Ma [Figure 5].

A total of 198 zircons were analysed from sample FR3_082a, Myrtle Springs Formation, with 176 passing filtering parameters. Grain ages range from 3451 ± 36 Ma to 807 ± 16 Ma, with a primary population peak c. 1000 Ma. Subordinate population peaks are present c. 2490 Ma, c. 1800 Ma, and c. 1280 Ma [Figure 5].

A total of 171 zircons were analysed from sample SF1, Stonyfell Quartzite, with 164 passing filtering parameters. Grain ages range from 3122 ± 35 Ma to 1536 ± 28 Ma, with a prominent primary population peak c. 1840 Ma. Minor population peaks are present at c. 2500 Ma, c. 2000 Ma, c. 1740 Ma, and c. 1590 Ma [Figure 5].

A total of 143 zircons were analysed from sample FRX_002, Saddleworth Formation (Minburra Quartzite Member), with 83 passing filtering parameters. Grain ages range from 2556 ± 40 Ma to 692 ± 15 Ma, with a primary population peak c. 1130 Ma. Subordinate population peaks are present c. 2470 Ma, and c. 1540 Ma [Figure 5].

Sample FR1_006_03, Saddleworth Formation, had low zircon yield. In total only 11 zircons were analysed with 9 passing filtering parameters. Grain ages range from 2815 ± 38 Ma to 1562 ± 27 Ma. Due to the limited number of analyses and significant spread in ages, the KDE forms a broad spectrum [Figure 5].

Sample FRX_001, a sample taken from a likely equivalent of the Gilbert Range Quartzite, had low zircon yield. Only 23 zircons were analysed with 17 passing filtering parameters. Grain ages range from 1682 ± 31 Ma to 988 ± 17 Ma, forming a predominant population peak at c. 1160 Ma [Figure 5].

A total of 113 zircons were analysed from sample ML_008, Mitcham Quartzite, with 93 passing filtering parameters. Grain ages range from 3746 ± 41 Ma to 726 ± 13 Ma, with a primary population peak c. 1080 Ma. Subordinate population peaks are present c. 1630 Ma, c. 1400 Ma, c. 930 Ma, and c. 740 Ma [Figure 5].

4.2 Umberatana Group

Sample FR3_111a, Fortress Hill Formation, had low zircon yield. This sample was collected from a very fine sandy lithology within a formation of mostly siltstone. A total of 19 zircons were analysed with 18 passing filtering parameters. Grain ages range from 2417 ± 67 Ma to 976 ± 15 Ma. Due to the limited number of analyses and significant spread in ages, the KDE forms a broad spectrum [Figure 5].

Sample FR3_089a, Mount Curtis Tillite, had low zircon yield. A total of 45 zircons were analysed over two analytical sessions, with 34 passing filtering parameters. Grain ages range from 2444 ± 25 Ma to 986 ± 18 Ma, with a predominant population peak c. 1160 Ma [Figure 5].

Sample FR3_088a, Balparana Sandstone, had extremely low zircon yield. A total of 9 zircons were analysed over two analytical sessions, with only 6 passing filtering parameters. Grain ages range from 1771 ± 24 to 944 ± 14 Ma. Due to the extremely limited number of analyses and significant spread in ages, the KDE forms a broad spectrum [Figure 5].

4.3 Wilpena Group

A total of 120 zircons were analysed for sample FR3_095a, Bonney Sandstone, with 102 passing filtering parameters. Grain ages range from 2752 ± 48 Ma to 610 ± 9 Ma, with a primary population peak c. 1120 Ma. Subordinate population peaks are present c. 2310 Ma, c. 1590 Ma, and c. 790 Ma [Figure 5].

An additional 15 zircons (the remainder on the mount) from sample 319 (Lloyd et al. 2020), Rawnsley Quartzite, were analysed during this study to gain some geochemical data for the zircons in this sample. All 15 passed filtering parameters with grain ages range from 1215 ± 14 to 949 ± 15 Ma. Due to the extremely limited number of analyses the KDE forms a broad spectrum with a central peak c. 1160 Ma [Figure 5].

An additional 96 zircons (the remainder on the mount) from sample 058 (Lloyd et al. 2020), Billy Springs Formation, were analysed during this study to gain some geochemical data for the zircons in this sample. A total of 73 analyses passed filtering parameters, with grain ages ranging from 2743 ± 40 Ma to 527 ± 8 Ma. A primary population peak is present c. 1580 Ma, with a secondary population peak c. 660 Ma [Figure 5].

4.4 Zircon trace element geochemistry

Most analyses resolved lanthanoid concentrations that are typical for zircons, with several orders-of-magnitude increase in concentration from light to heavy elements, a slight negative deviation in europium (Eu), and a positive deviation in cerium (Ce) [Figure 6]. Two analyses (FR3_095a – 032, and FR3_089a - 034) have lanthanoid concentrations atypical of zircon, with overall positive (based on ionic radii) slopes (λ_1 of +9.03, and +3.72) due to highly elevated light lanthanoids (La to Nd). Overall, the lanthanoid pattern for both analyses have a concave-up shape (+λ_2) with mid to heavy lanthanoid concentration increasing as would normally occur in zircon. Major element percentages,

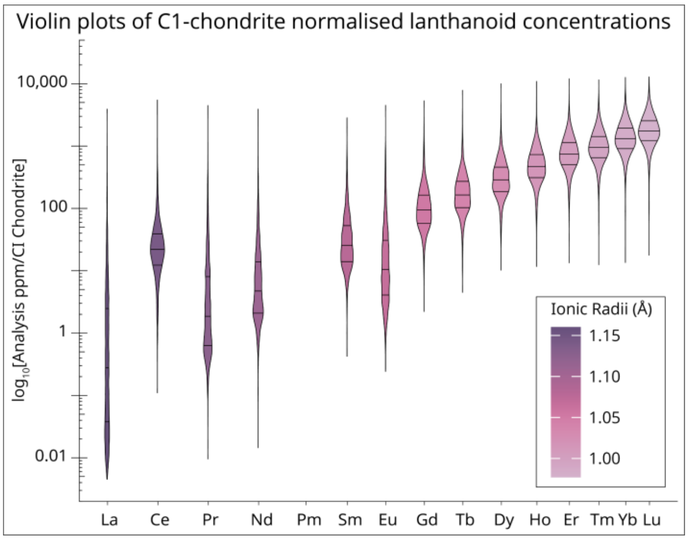

Figure 6 – Violin plots of CI chondrite (O'Neill 2016) normalised lanthanoids for all filtered zircon analysed in this study. X-axis is spaced by ionic radii (Shannon 1976) and ordered by atomic number. Black lines across the fill of each plot represent the 0.25, 0.5, and 0.75 quantiles. Bandwidth of the density estimates is calculated using the Botev algorithm from the Provenance package (Vermeesch et al. 2016).

~13.25 wt% and ~18.57 wt% silicon, suggest these two analyses are zircon, and CL images also support this. It is likely these two analyses have gone through complicated zones of inclusions not visible on the CL images of the grain surfaces. Another noticeable anomaly is present on Figure 7, where one Ce* c. 1700 Ma is significantly greater than any other analysis. This analysis is FR3_036 – 016 and has a Ce* value of ~ 230,000. This is anomalous as both La and Pr were below detection limit, and the zircon has a low average lanthanoid concentration (λ_0 of -0.5495). As such, this Ce* value is considered unreliable.

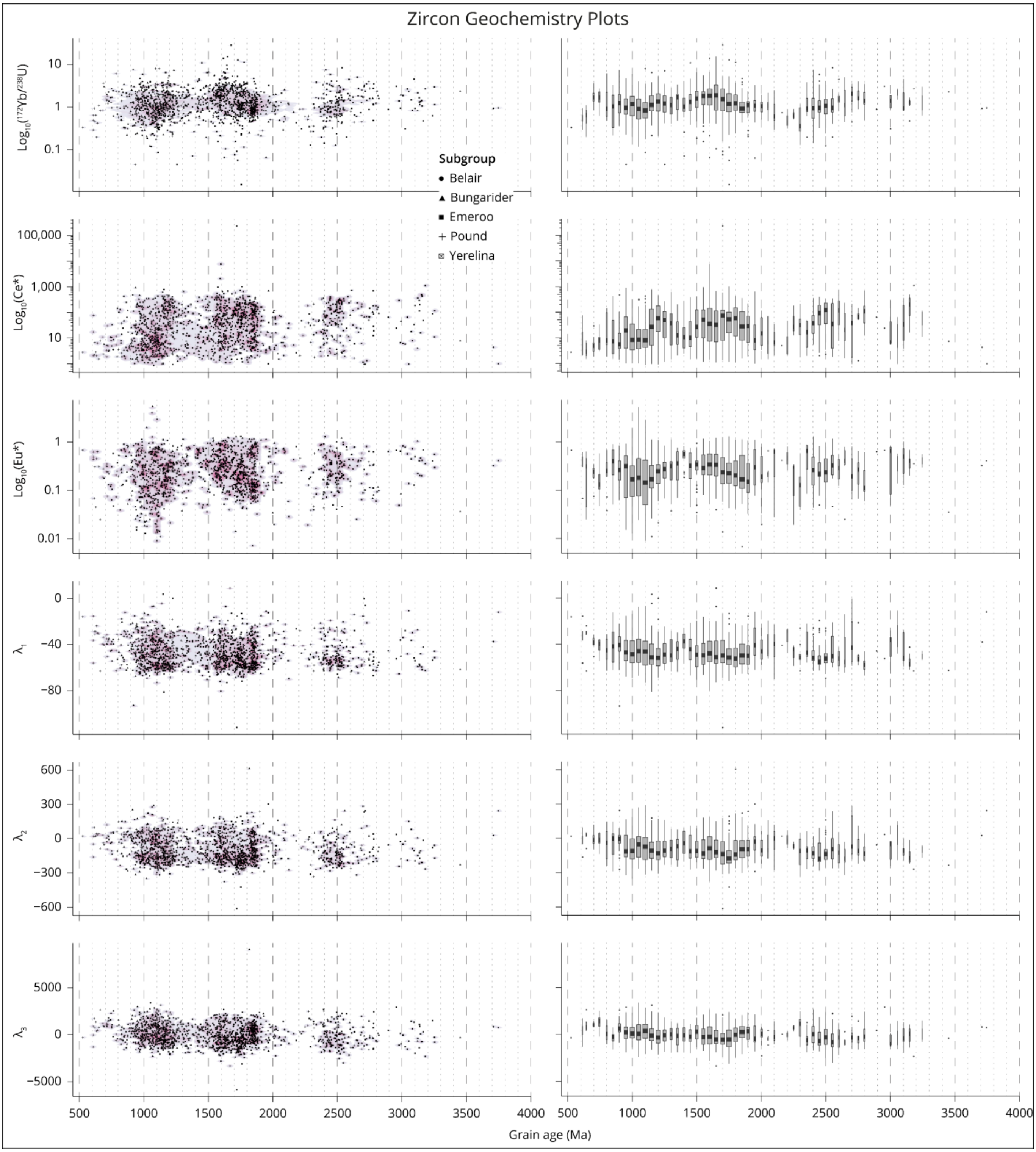

Figure 7 – Key zircon geochemistry plots for zircon analysed in this study. Left: Scatter plots underlain with 2D density estimation. Right: 50-million-year binned boxplots with width scaled by the count of values in the bin. Top to bottom: Yb/U, Ce*, Eu* and λ1–3. λ1–3 are measures of lanthanoid pattern shapes, with λ1–3 representing the linear slope, quadratic slope and cubic slope respectively. Ce*, Eu* and λ1–3 are calculated using BLambdaR (Anenburg & Williams 2021).

5 Discussion

5.1 Zircon trace element geochemistry

A simple U/Yb against Y plot can be used to infer continental or oceanic affinity for zircon generation (Grimes et al. 2007; Grimes et al. 2015). Most zircons analysed in this study are inferred to have been generated in continental crust [Figure 8], with a small number of younger zircons suggestive of oceanic affinity. C1 chondrite normalised (O'Neill 2016) concentrations of lanthanoids are generally typical of zircon [Figure 6] with a positive pattern slope (increasingly negative λ1 values) from light to heavy lanthanoids, a positive cerium anomaly, and negative europium anomaly (Hoskin & Ireland 2000; Hoskin & Schaltegger 2003). Nearly all zircons have a Th/U >0.07 and are generally inferred to be originally generated as magmatic rather than metamorphic zircon (Collins et al. 2004; Rubatto 2002). There are no significant trends in lanthanoid pattern slope or curvature [Figure 7], denoted as λ1 (linear slope), λ2 (quadratic slope), and λ3 (cubic slope) (Anenburg 2020), with time or sample. Both Eu and Ce anomalies (denoted by Eu* and Ce*) show a significant spread through time. However, an increasing number of zircons c. 1000 Ma show low (i.e., deep) Eu* anomalies with greater data spread. Additionally, sub 1000 Ma zircons show a minor trend towards higher Eu*, and correspondingly lower Ce*, suggesting zircon growth in competition with plagioclase, and not reflective of magma oxidation state (Verdel et al. 2021).

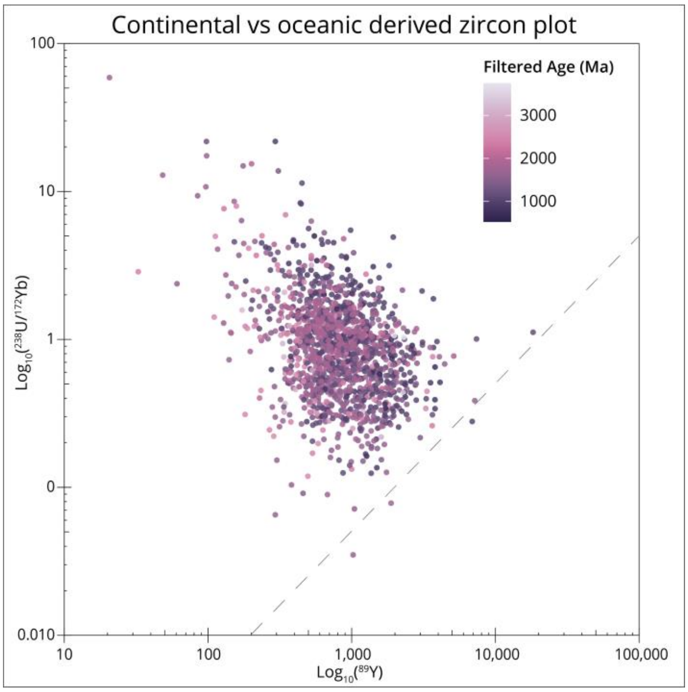

Figure 8 – Plot based on (Grimes et al. 2007) used as an indicator of zircon crustal origin. This plots Y against U/Yb, with the dashed reference line dividing the "oceanic" (below line) and "continental" (above line) fields. Most data plot above the reference line, suggesting zircon formation mostly in crust of continental affinity. Coloured by filtered age where light is older and darker is younger.

5.2 Provenance and maximum depositional ages

5.2.1 Maximum depositional ages (MDAs)

A summary of MDAs from this study and published literature is presented along with the stratigraphic table in Figure 3. Sample locations are shown in Figure 1 with Figure 2 showing regional geographic areas. As highlighted in the results, maximum depositional ages quoted here differ from the youngest grain quoted in the results section. A conservative method is employed so that only high confidence (within 2% of concordance) grain age determinations are considered, and the oldest of the three derived ages for an individual grain is quoted.

5.2.1.1 Burra Group

Several age constraints for the samples from the Burra Group exist. A limit defining the oldest age possible for Burra Group rocks is 802 ± 10 Ma from the Rook Tuff within the upper Curdimurka Subgroup, although the reliability of this age is questioned (Lloyd et al. 2022b, preprint). Within the Burra Group an age of 788 ± 6 Ma has been determined (Armistead et al. 2020) for the Boucaut Volcanics. While the exact stratigraphic position of the Boucaut Volcanics remains unresolved (Lloyd et al. 2020), it lies within the lower Burra Group, likely at the top of the oldest Emeroo Subgroup. This is based on the similar age, 794 ± 4 Ma (Preiss et al. 2009), obtained for a syndepositional volcanic porphyry within the Skillogalee Dolomite of the overlying Mundallio Subgroup. Additionally, an intrusive bimodal volcanic sequence only preserved in diapiric breccia of the underlying Callanna Group, the Oodla Wirra Volcanics, has an age of 798 ± 5 Ma/799 ± 4 Ma (Fabris et al. 2005). The youngest limit for deposition of the Burra Group is poorly constrained as no volcanogenic sequences have been found to date in the upper Burra Group. The best constraint to date are MDAs c. 730 Ma obtained for both the Gilbert Range Quartzite (Keeman et al. 2020; Lloyd et al. 2020) and Mitcham Quartzite (van der Wolff 2020) of the Belair Subgroup. These MDAs, combined with those of the Sturt Formation. c. 714 Ma and c. 666 Ma (Lloyd et al. 2022d, preprint), closely align with the time band defined globally for the *Sturtian glaciation* (Lloyd et al. 2022d, preprint; Rooney et al. 2015). As such, it is likely the younger limit for timing of deposition of the Burra Group is c. 714 Ma.

Emeroo Group samples the Humanity Seat Formation (FR3_036), Blue Mine Conglomerate (FR3_035), Opaminda Formation (FR2_396), Wortupa Quartzite (FR3_010), and Copley Quartzite (FR3_123, FR2_002_01, & FR2_004_01) were deposited between 802 ± 10 Ma and c. 790 Ma. The obtained MDAs for these samples were 1558 ± 35 Ma, 1081 ± 19 Ma, 1374 ± 21 Ma, 857 ± 18 Ma, 892 ± 33 Ma, 1218 ± 31 Ma, and 838 ± 13 Ma respectively. All of these MDAs are older than their expected depositional ages (<802 ± 10 Ma, >c. 790 Ma).

Bungarider and Belair Subgroup samples were deposited post Mundallio Subgroup, c. 790 Ma, and likely before c. 714 Ma, with the Belair Subgroup being the younger of the two. The Myrtle Springs Formation (North Flinders Ranges) sample, FR3_082a, has an MDA of 810 ± 42 Ma (^{207}Pb/^{235}U), however both the ^{206}Pb/^{238}U and ^{207}Pb/^{206}Pb ages agree at 807 ± 16 and 807 ± 37 Ma, respectively, which would be used by many as the MDA (note that our definition is extremely conservative). The Saddleworth Formation sample, FRX_002 (South Flinders Ranges), has an MDA of 956 ± 16 Ma, and while data is extremely limited, sample FR1_006_03 (North Mount Lofty Ranges), has an MDA of 1592 ± 36 Ma. The MDA derived for sample FRX_002 is significantly older than the youngest grain quoted in the results section above, this is due to the more conservative criteria used here to define the MDA (i.e., within 2% of concordance). The final Bungarider Subgroup sample is from the Stonyfell Quartzite, SF1 (South Mount Lofty Ranges), and has an MDA of 1585 ± 25 Ma. These are all older than expected depositional ages for the Bungarider Subgroup rocks.

Sample FRX_001 (South Mount Lofty Ranges) is from a sedimentary rock thought to be equivalent of the Gilbert Range Quartzite. Zircon yield was low for this sample with an MDA of 1101 ± 17 Ma obtained. Gilbert Range Quartzite sample, FR1_003_01 (North Mount Lofty Ranges), has an MDA of 869 ± 14 Ma. The final Burra Group sample in this study comes from the Mitcham Quartzite, sample ML_008 (South Mount Lofty Ranges). This was a second run on the sample to add additional data and for verification purposes of the MDA obtained in van der Wolff (2020). An MDA of 734 ± 42 Ma ($^{207}Pb/^{235}U$) was obtained for the analyses in this study. Comparatively, the MDA quoted by van der Wolff (2020) was 720 ± 21 Ma ($^{206}Pb/^{238}U$). The equivalent $^{206}Pb/^{238}U$ age for the grain in this study is 730 ± 14 Ma and the $^{207}Pb/^{206}Pb$ age is 732 ± 41 Ma. The calculated $^{207}Pb/^{235}U$ age from van der Wolff (2020) is 732 ± 61 Ma and the $^{207}Pb/^{206}Pb$ age is 754 ± 51 Ma.

5.2.1.2 Umberatana Group

The three samples from the upper Umberatana Group (Yerelina Subgroup) were deposited during the onset (FR3_0111a, Fortress Hill Formation), maximum (FR3_089a, Mount Curtis Tillite), and deglaciation (FR3_088a, Balparana Sandstone) of the *Marinoan glaciation*. All samples had low zircon yield, with FR3_088a being extremely low; the sample was a highly silicified very coarse sand arkose. The MDA for sample FR3_0111a is 977 ± 36 Ma, for sample FR_089a is 1032 ± 36 Ma, and for sample FR3_088a is 946 ± 31 Ma.

No firm radiometric age constraints have been determined from within the Adelaide Superbasin on the Yerelina Subgroup representing the *Marinoan Glaciation*. Rose et al. (2013) obtained an MDA of 641 ± 5 Ma for the stratigraphically correlative Whyalla Sandstone on the Stuart Shelf. Additionally, Re–Os ages have provided a minimum age estimate for the interglacial Tapley Hill Formation of the Nepouie Subgroup c. 642 Ma (Kendall et al. 2006), with a maximum constraint from detrital zircon of 654 ± 13 Ma (Lloyd et al. 2020). The Nepouie Subgroup is overlain by the Upalina Subgroup, which in turn underlies the Yerelina Subgroup, as such there is likely a reasonable amount of time between this constraint and the initial deposition of the Yerelina Subgroup. Globally, the *Marinoan glaciation* is constrained to a younger limit c. 635 Ma (Calver et al. 2013; Rooney et al. 2015), while the older limit is not well defined. As such, the expected depositional age of the Yerelina Subgroup should be c. 645 to c. 635 Ma.

5.2.1.3 Wilpena Group

Sample FR3_095a is from the upper portion of the Bonney Sandstone. An MDA of 611 ± 20 Ma was obtained for this sample. Previously an MDA of 579 ± 32 Ma (Lloyd et al. 2020) was obtained for the Bonney Sandstone.

Additional zircons were analysed from samples 058 (Billy Springs Formation) and 319 (Rawnsley Quartzite) of Lloyd et al. (2020) in order to gain some trace element geochemistry for these samples. Only a few zircons were remaining on sample 319, with an MDA of 1091 ± 22 Ma obtained from this limited data set. The MDA for sample 058 for this analytical session is 640 ± 26 Ma. Previous MDAs for these formations are 570 ± 23 Ma, and 564 ± 25 Ma respectively. No grains younger than 640 ± 26 Ma in sample 058 for this analytical session are within 2% of concordance and thus are not considered reliable for MDA determination.

5.2.2 Provenance

Archaean zircons present in the detrital spectra [Figure 5] of all samples are consistent with being derived from local sources within the Gawler Craton and recycling of detrital material from the Willyama Supergroup of the Curnamona Province [Figure 9]. Numerous magmatic events occurred within the Gawler Craton c. 3250 Ma, 3150 Ma, 2820 Ma, and 2560–2470 Ma, and inherited/detrital zircon up to 3400 Ma are present throughout the terrane (Fanning et al. 2007; Fraser et al. 2010; Fraser & Neumann 2010; Jagodzinski & McAvaney 2017; Jagodzinski et al. 2020; McAvaney 2012; Reid & Jagodzinski 2011; Williams, MA & Reid 2021). The Willyama Supergroup in the Curnamona Province contains detrital populations ca. 3000–2980 Ma, and ca. 2680–2650 Ma (Page et al. 2005), while their initial origin may the North Australian Craton (e.g., Barovich & Hand 2008). All but one zircon of Archaean age is feasibly attributed to these local sources. One zircon present within the Mitcham Quartzite has an Eoarchaean age of c. 3746 Ma. The time resolved analysis of this zircon revealed two distinct zones of Pb and Pb/Th ratios, and REE concentrations. Both integration periods resolve ages c. 3700 Ma, with the latter part of the signal (~10s) resolving a nearly perfectly concordant measurement. Regardless of this complexity that is likely a result of inclusions, the age of this zircon can be confidently resolved as being mid-Eoarchaean. Zircons of this age are extremely rare throughout the sedimentary rocks of the Adelaide Superbasin with few potential sources, none locally (Lloyd et al. 2020).

Palaeoproterozoic zircons are ubiquitous throughout all samples but become increasingly less common up stratigraphy [Figure 5]. The first consistently recorded population is late Archean to early Palaeoproterozoic, c. 2510–2400 Ma. These ages correlate well with the Sleaford Orogeny of the Gawler Craton (Reid et al. 2014). The most prominent Palaeoproterozoic zircon population occurs c. 1800–1600 Ma. Both the Gawler Craton and Curnamona Province [Figure 9] record abundant zircon of this age either as magmatic, metamorphic, or detrital components (Barovich & Hand 2008; Belousova et al. 2009; Fanning et al. 2007; Fraser & Neumann 2010; Jagodzinski & Fricke 2010; Jagodzinski & McAvaney 2017; Jagodzinski et al. 2020; McAvaney 2012; Meaney 2012; 2017; Morrissey et al. 2019; Reid & Hand 2012; Reid & Jagodzinski 2011; Reid et al. 2019; Reid & Payne 2017; Swain et al. 2005). Another possible source is the Yavapai-Mazatzal Province of Laurentia due to similarities in ages and proximity to the Adelaide Superbasin within some Rodinia reconstructions (Brookfield 1993; Dalziel 1991; Goodge et al. 2008; Hoffman 1991; Karlstrom & Bowring 1988; Karlstrom et al. 1999; Moores 1991; Wingate et al. 2002).

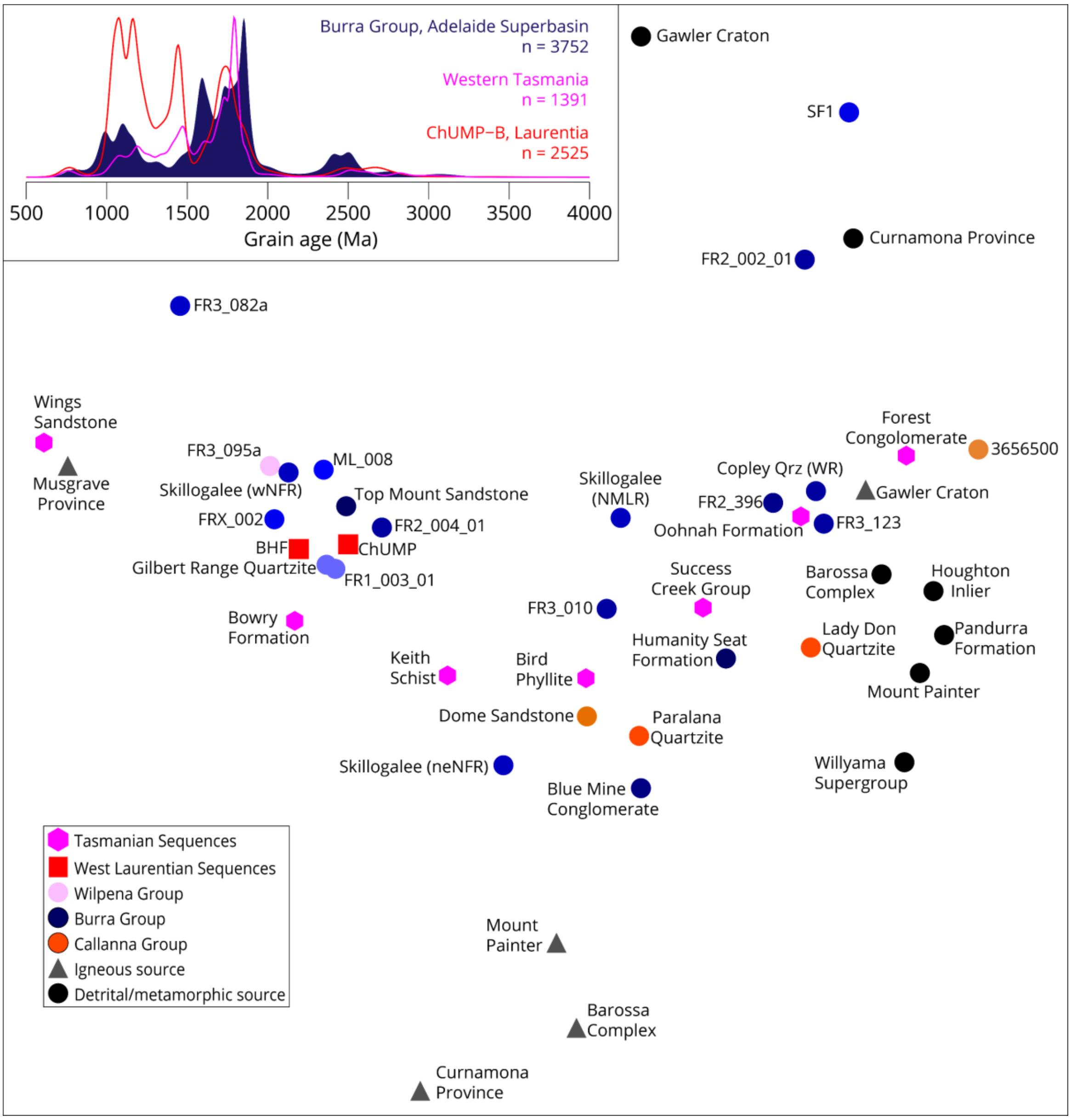

Figure 9 – A) Overlain KDEs of Tonian sequences of the Adelaide Superbasin (Burra Group; this study, Keeman et al. 2020; Lloyd et al. 2020; van der Wolff 2020), western Laurentia (Chaur, Uinta Mountain, middle Pahrump Groups–Buffalo Hump Formation correlated rocks [ChUMP-B]; Brennan et al. 2021; Dehler et al. 2017) and the Western Tasmania Terrane (Mulder et al. 2018a; Mulder et al. 2020). B) Non-metric multidimensional scaling plot of samples analysed (n > 40) in this study (blue coloured circles, pink circle) with data from underlying Adelaide Superbasin rocks (orange circles; Brotodewo et al. 2021; Lloyd et al. 2020), potential correlative formations in Tasmania (magenta hexagons), western Laurentia (red squares), and potential source regions for the Adelaide Superbasin rocks (black and grey circles and triangles). This plot shows relative similarity of all data to each other and are intended as a visual guide. Points that closer together suggest greater similarity. For data of the Adelaide Superbasin, the lightness of colour corresponds to stratigraphic position, i.e., lighter shade are younger rocks. Axes are omitted as the algorithm used produces normalised values with no physical meaning and can be safely removed. Produced using IsoplotR (Vermeesch 2018).

Mesoproterozoic zircon c. 1580 Ma forms a generally significant population [Figure 5] in older samples from the far northeast of the basin [Figure 1], those in close proximity to the Mount Painter Inlier. It also forms a significant component of the Belair Subgroup samples in the far south of the basin [Figure 1]. These are feasibly attributed to local derivation [Figure 9] from the Ninnerie Supersuite and Radium Creek Group (Armit et al.

2014; Wade, CE 2011), with additional potential sources being the Gawler Range Volcanics, Hiltaba Suite, and Barossa Complex of the Gawler Craton (Fanning et al. 2007; Meaney 2017). A second Mesoproterozoic zircon population is present c. 1100 Ma. While generally absent from the older stratigraphic units [Figure 5, Figure 1], it becomes predominant in sample FR2_004_01 from the very top of the Copley Quartzite in the transitional section to the overlying Skillogalee Dolomite. This is a notable change in population spectra from sample FR2_002_01 [Figure 5, Figure 9], which was sampled mid-Copley Quartzite in the same stratigraphic section. While Stenian zircon is almost absent in the two additional Copley Quartzite samples from this study [Figure 5], and from the samples presented in Lloyd et al. (2020), this is most likely as result of stratigraphic height of sampling. This Stenian population is also present, but not as predominant in the coeval Wortupa Quartzite. In the overlying Skillogalee Dolomite, there are significant variations in the population spectra [Figure 5, Figure 9] dependant on sample location. In the far northeast of the basin, the Calymmian population (c. 1580 Ma) remains the principal signature with a minor contribution from late Mesoproterozoic zircon, while in the Willouran Ranges to the northwest, Stenian zircon (c. 1100 Ma) are abundant. To the south, roughly in the middle of the basin, Stenian zircon are almost entirely absent from the Kooringa Member of the Skillogalee Dolomite. The Myrtle Springs Formation sample from the middle (west–east) of the North Flinders Ranges [Figure 1, Figure 2] forms a single population peak centred on the Stenian-Tonian boundary, with only minor but consistent contributions from older source material [Figure 5]. In the south of the basin this influx of latest Mesoproterozoic zircon occurs in a higher stratigraphic position, between the lower Bungarider Subgroup (Stonyfell Quartzite) and Belair Subgroup (Mitcham Quartzite) [Figure 5]. The Saddleworth Formation samples from the middle of the basin appear to reflect these trends [Figure 5]. The rather significant changes in detrital zircon population spectra in the mid to upper Burra Group [Figure 9] strongly suggest an increasingly restricted, but more distal source region, the Musgrave Province (Howard et al. 2015; Smithies et al. 2008; Smithies et al. 2011; Smits et al. 2014; Wade, BP et al. 2008), as has been inferred in past studies (Keeman et al. 2020; Lloyd et al. 2020). One alternate source is the Albany-Fraser Orogen of Western Australia (Spaggiari et al. 2015). However, this would require transport across the Gawler Craton at the same time as deposition was occurring in the western Officer Basin (Zi et al. 2019). In addition, coeval, c. 750–720 Ma, uplift of the Musgrave Province has been interpreted to occur (Howard et al. 2015) and, the abrupt up-sequence spectra change in the two Copley Quartzite samples [Figure 5, Figure 9] from the Copley area [Figure 2] suggests that the Gawler Craton somewhat shut off as a source region, effectively precluding the Albany–Fraser Orogen as a source. Antarctic sources are also possible, where the late Mesoproterozoic/early Tonian zircon in the Palaeozoic Lachlan Orogen is thought to be derived from (Squire et al. 2006). A distinguishing feature of these Lachlan Orogen zircons is the significant amount of <1050 Ma zircon, these are more characteristic of parts of East Antarctica such as the Tonian Oceanic Arc Super Terrane (TOAST, Jacobs, Joachim et al. 2015; Jacobs, J. et al. 2017) and the Rayner Complex (Fitzsimons 2000). The Myrtle Springs Formation, Mitcham Quartzite, and Gilbert Range Quartzite samples appear to support this [Figure 5]. The South Tasman Rise is another possible source for Stenian zircon, c. 1120 Ma (Fioretti et al. 2005), as is the hypothesised Precambrian keel of Zealandia (Turnbull et al. 2021).

Tonian zircon are almost entirely absent from the Emeroo Subgroup stratigraphy in the north of the basin, and are absent from all Emeroo to mid-Bungarider Subgroup stratigraphy in the far south of the basin near Adelaide [Figure 5, Figure 1] so far reported (this study; van der Wolff 2020). The presence of Neoproterozoic zircon in Burra Group sequences generally coincides with the introduction of Stenian zircon, the exception being the Kooringa Member of the Skillogalee Dolomite [Figure 5] where syndepositional magmatism is recorded (Preiss et al. 2009). For the most part, Tonian zircons within the Burra Group sequences are c. 1000–780 Ma in age, with a minor amount of zircon with ages 760–730 Ma in the Mitcham Quartzite [Figure 5]. Zircon c. 830–780 Ma is probably derived locally from the early magmatism recorded in the Callanna Group, and lower Burra Group (Armistead et al. 2020; Fanning et al. 1986; Preiss et al. 2009; Preiss et al. 2008; Wingate et al. 1998). Zircons with ages between c. 1000 Ma and 890 Ma, and c. 760–730 Ma are more enigmatic. While earlier zircon c. 1000 Ma may be attributable to the Musgrave Province where some bimodal magmatism is recorded (Howard et al. 2015), the reasonably significant number of concordant zircon between 980 and 900 Ma is much more difficult to reconcile with current data from the Musgrave Province and these age determinations are not likely to be an artefact of analytical or statistical techniques for determining ages. Zircon of crystallisation age between c. 760–730 Ma found in Burra Group sedimentary rocks are, to date, only found in the Mitcham Quartzite. While a few grains of these ages are in the dataset for the Saddleworth Formation they are likely to be artefacts of radiogenic Pb loss or inclusions impacting the U–Pb age determinations and are not considered particularly dependable. Within Proterozoic Australia few sources of zircon c. 760–730 Ma are known to exist. Poorly constrained age determinations of c. 765 Ma were obtained from mafic volcanics of the Polda Basin just to the west of the Adelaide Superbasin via K–Ar dating of plagioclase (Flint et al. 1988). In the southwestern Pilbara Region of Western Australia an age of 755 ± 3 Ma was determined for the Mundine Well Dolerite by U–Pb analysis of zircon and baddeleyite (Wingate & Giddings 2000), while the Keene Basalt in the western Officer Basin has been dated at c. 754 Ma, and c. 752 Ma by $^{40}Ar/^{39}Ar$ determinations of plagioclase and pyroxene respectively (Zi et al. 2019). An age of c. 731 Ma has been resolved from zircon of the Mud Tank Carbonatite in the Strangways Range, Northern Territory (Black, Lance P. & Gulson 1978; Gain et al. 2019). Mulder et al. (2020) summarised several Tonian magmatic ages from Tasmania, these being c. 780 Ma, 775 Ma, 760 Ma, 748 Ma, and 733 Ma; however, in their model western Tasmania is located at the south-eastern edge of East Antarctica. Given the low abundance of these zircon in the Mitcham Quartzite, and lack of zircon of this age in northern samples [Figure 5] it would suggest that they are not derived from the north-westerly sources, and are more likely derived from either local, low volume magmatism, or more distal southerly sources, potentially western Tasmania.

South China and Tarim contain magmatic records of Tonian zircon c. 1000 Ma to c. 700

Ma (Cawood et al. 2020; Cawood et al. 2018; Hui et al. 2021; Lan et al. 2015; Shu et al. 2021; Wu et al. 2021) and have both been previously invoked as “missing-link” models within central Rodinia between Australia–Laurentia (Li et al. 2008; Li et al. 1995; Wen et al. 2017; Wen et al. 2018); however, we do not consider these to be viable source regions for the Adelaide Superbasin for a number of reasons. A growing consensus of researchers (Cawood et al. 2020; Eyster et al. 2019; Park et al. 2021; Wu et al. 2018; Wu et al. 2021; Zhang et al. 2019; Zhao et al. 2021; Zheng et al. 2020; Zhou et al. 2021) have independently drawn conclusions that these two terranes are either on the periphery of or detached from Rodinia. This is supported by multiple lines of geologic evidence including palaeomagnetic studies, detrital zircon studies, and more wholistic tectonic evolution models for these terranes involving multiple methods (e.g., Merdith et al. 2019).

Cryogenian to Ediacaran zircon are abundant in the Yerelina and Pound Subgroup samples, and have been addressed in Lloyd et al. (2020). The results obtained in this study, even though generally limited in number, conform to earlier results [Figure 5], and the ultimate source of these zircon remains enigmatic aside from some local magmatism c. 660 Ma (Cox et al. 2018) and c. 580 Ma (Black, L. P. 2007).

Interestingly, both the Skillogalee Dolomite samples (Lloyd et al. 2020) from the Willouran Ranges and Myrtle Springs Formation sample have a considerable number of sub 1030 Ma zircon, with the most predominant population peak c. 1000–990 Ma for both samples [Figure 5]. Additionally, Mesoproterozoic zircon in the Myrtle Springs Formation sample appears to not be reflect the typical bimodal (c. 1220–1150 Ma & 1090–1040 Ma) Musgrave Province signature (Howard et al. 2015; Johansson et al. 2022). While not precluding detritus derived from the Musgrave Province, it does suggest an alternate source may have been involved. Given the consistency of zircon populations in Emeroo to mid-Bungarider Subgroup in the very south of the basin (van der Wolff 2020), and the lack of late Mesoproterozoic to early Tonian zircon in the Skillogalee Dolomite from the North Mount Lofty Ranges [Figure 5], it effectively rules out a southerly source for these. This suggests an unrecognised source to the north or northeast of the Adelaide Superbasin. Contrastingly, younger Pound Subgroup zircon populations [Figure 5] are more easily reconciled as being primarily derived from the Musgrave Province [Figure 9] with other additional sources, likely to the south, accounting for Cryogenian to Ediacaran zircon populations (Lloyd et al. 2020).

5.3 Comparison to Tasmanian and Laurentian sequences

Along with North China and eastern Proterozoic Australia, both the Western Tasmania Terrane (WTT) and western Laurentia are witness to the opening of the proto-Pacific Ocean during the breakup of Rodinia (Brennan et al. 2021; Merdith et al. 2021; Mulder et al. 2020). As such, the stratigraphic sequences recorded in these rift basins are crucial to better understanding the configuration of these continental blocks within the heart of Rodinia. Mulder et al. (2020) suggest three potential positions for the WTT at c. 730 Ma, one against southeast East Antarctica, and two against western Laurentia. A comparison of the detrital zircon spectra of time-equivalent sedimentary sequences in these terranes provides insights into their relative positions and links. The coeval sedimentary sequences of the Burra Group in the WTT are the Wings Sandstone, Bowry Formation, Keith Schist, Forest Conglomerate, Bird Phyllite, Success Creek Group, and Oonah Formation (Mulder et al. 2018a; Mulder et al. 2020). In western Laurentia the coeval sequences are the ChUMP-B (Chaur, Uinta Mountain, middle Pahrump Groups–Buffalo Hump Formation) correlated rocks (Brennan et al. 2021; Dehler et al. 2017). The more nuanced complexity of the geological history and detrital zircons of these rocks from the WTT and western Laurentia are detailed in their respective publications. The combined detrital zircon distributions of the late Tonian ChUMP-B, WTT, and Burra Group rocks are overlain on the inset of Figure 9, and while they do show significant similarities, some key differences appear. The most obvious differences are the position of the latest Palaeoproterozoic peaks, the relative lack of earliest Mesoproterozoic zircon in the WTT and ChUMP-B spectra, and the position of the latest Stenian to early Tonian peaks. In the datasets available, WTT rocks show remarkable similarity to the ChUMP-B populations, closely following the general trends, albeit in different relative proportions. The combined spectra suggest, that overall, WTT has a stronger affinity with western Laurentia than it does southeast Proterozoic Australia, but all terranes share some similar aged sources. However, the individual WTT sequences plot (on an MDS) with an inverse stratigraphic relationship relative to similarity of the western Laurentian data—that is they become increasingly dissimilar up sequence [Figure 9]. The Oonah Formation and Forest Conglomerate are suggested (Mulder et al. 2020) to recycle underlying Rocky Cape Group that is thought to correlate with the Unkar Group in southwestern Laurentia (Mulder et al. 2018b). This is a sensible finding, given the overall change to older detrital zircon population up sequence as would occur in an unroofing scenario. However, additional, igneous and metasedimentary sources from the Mawson Continent (Williams, MA et al. 2018) may also be involved as these closely align with the zircon distributions recorded. This observation, combined with the relative lack of Stenian zircon that are abundant in upper ChUMP-B rocks, would suggest that the WTT remained on the western side of the proto-Pacific and would allow for the late Tonian magmatism recorded in the WTT to be a potential source of the rare, enigmatic c. 760–730 Ma zircons found in the Belair Subgroup of the Adelaide Superbasin. Contrastingly, generally younger Burra Group rocks show greater similarity [Figure 9] to the ChUMP-B strata; however, this is likely due to the greater Stenian zircon populations present in the upper Burra Group derived from the Musgrave Province, and a potentially intervening terrane to the north/northeast of the basin as discussed prior rather than a shared source in the very latest Tonian.

Unfortunately, no detrital zircon data from the Burra Group rocks in the far east of the basin have been obtained to date, and little is known of what lies beneath the Warburton Basin to the north. This significantly hinders the ability to understand the links between eastern Proterozoic Australia and western Laurentia or any intervening terrane.

5.4 Tectonic and palaeogeographic implications

It is evident that tectonics played a significant role during the deposition of the Burra Group. Significant and rapid changes in thickness and lithology [Figure 4], both vertically and laterally throughout the basin (Preiss 1987; 1993; 2000; Uppil 1980), suggest the development of numerous half-graben depocentres, as do abrupt changes in detrital zircon populations [Figure 9, Figure 5] up sequence. In the north of the basin there is abrupt change in detrital zircon spectra [Figure 9, Figure 5] with significant decrease in detrital zircon characteristic of the Gawler Craton and a corresponding increase in zircon thought to be derived from the Musgrave Province. This transition in source occurs at the Emeroo–Mundallio Subgroup boundary and suggests the uplift of rift shoulders c. 800–790 Ma. Interestingly detrital zircon ages shift to a latest Stenian to early Tonian population in the Myrtle Springs Formation [Figure 5] of the Bungarider Subgroup. Currently the source of these zircon is unknown but is likely to be from the north or northeast. This is based upon the uniformity of equivalent strata in the south of the basin reflecting purely local derivation from older Palaeoproterozoic to early Mesoproterozoic sources (van der Wolff 2020), and the sequences in the middle of the basin reflecting the same observation, with the addition of c. 790–780 Ma from local sources.

The same abrupt transition in detrital zircon spectra [Figure 9, Figure 5] occurs much later in the southern and middle areas of the basin during deposition of the upper Bungarider Subgroup (Saddleworth Formation) to lower Belair Subgroup (Mitcham Quartzite). These observations suggest a southward propagation of the rift system in the Adelaide Superbasin, with main pulses of extension occurring c. 790 Ma in the northern to middle areas (and likely eastern) of the basin, and sometime around 750–730 Ma in the southern and middle areas of the basin. The older c. 790 Ma extension has a known magmatic record within the Adelaide Superbasin (Armistead et al. 2020; Preiss 1987; 2000; Preiss et al. 2009), while the younger extension appears to be amagmatic thus far. It is also likely that rift shoulders were well developed by ~750–730 Ma for the entire Adelaide Rift Complex as Palaeoproterozoic and older zircon characteristic of the Gawler Craton are only present in relatively minor amounts in the upper Burra Group sedimentary rocks.

These findings are supportive of an overall southward progressing rift system along the eastern margin of late Proterozoic Australia–East Antarctica, consistent with palaeogeographic and tectonic models of Merdith et al. (2021) and Mulder et al. (2020), and a likely continuation of the rift basin system under the modern day Trans-Antarctic Mountains (Goodge 2020).

6 Conclusions

Detrital zircon spectra from the late Tonian sedimentary rocks of the Adelaide Superbasin record a southward progressing rift system with abrupt changes in zircon populations and the sedimentology of these sequences suggestive of tectonic controls on sediment input and the development of depocentres. Key outcomes of this research are:

- Significant increase in the quantity and diversity of Burra Group detrital zircon data—1392 analyses
- Additional contribution to Yerelina and Pound Subgroup detrital zircon data—304 analyses
- Revised maximum depositional constraint on the Mitcham Quartzite and upper Belair Subgroup—734 ± 42 Ma
- Support for well-developed rift shoulders in the Adelaide Rift Complex by c. 730 Ma
- Southward propagation of the rift basin by extension in two main pulses
    - c. 790–780 Ma in the north and middle of the Adelaide Superbasin
    - c. 750–730 Ma in the south and middle of the Adelaide Superbasin
- Possibility of unrecognised source of c. 1000–900 Ma zircon to the north, or northeast of the basin

Funding

The Geological Survey of South Australia and the MinEx CRC funded this research. This research was supported by an Australian Government Research Training Program (RTP) Scholarship awarded to JCL.

Data Availability

Complete data for this publication are freely available for download from Figshare at the following links. These datasets contain all the U–Pb geochronology data, trace element data, and basic sample metadata.

Zircon and NIST standards data for all analytical sessions: https://doi.org/10.6084/m9.figshare.18131432 (Lloyd et al. 2022c)

Burra Group, Yerelina Subgroup, and Pound Subgroup detrital zircon data (this study): https://doi.org/10.6084/m9.figshare.19150607 (Lloyd et al. 2022a)

Zircon CL images: https://doi.org/10.6084/m9.figshare.19181024

Code Availability

R code used to generate the zircon geochemistry plots is available on GitHub at https://github.com/jarredclloyd/zircon-trace-element-plots

CRediT author statement

Jarred C. Lloyd: Conceptualisation, investigation, writing - original draft, writing - review & editing, methodology, formal analysis, data curation, visualisation. **Alan S. Collins:** Conceptualisation, funding acquisition, supervision, investigation, writing -

review & editing. **Morgan L. Blades:** Investigation, writing - review & editing. **Sarah E. Gilbert:** Formal analysis, methodology, investigation, writing - review & editing. **Kathryn J. Amos:** Conceptualisation, funding acquisition, supervision, writing - review & editing.

Acknowledgements

We acknowledge the Adnyamathanha, Arabana, Banggarla, Kaurna, Kokatha, Kuyani, Ngadjuri and Nukunu Peoples as the Traditional Owners and Custodians of the land on which this research is conducted. We acknowledge and respect their deep feelings of attachment and spiritual relationship to Country, and that their cultural and heritage beliefs are still as important to the living people today.

The authors acknowledge the instruments and scientific and technical assistance of Microscopy Australia at Adelaide Microscopy, The University of Adelaide, a facility that is funded by the University, and State and Federal Governments. Particular thanks to Aoife McFadden for their assistance with CL imaging.

We also thank Dr Wolfgang Preiss (Geological Survey of South Australia; University of Adelaide) for sharing his expertise on the Adelaide Superbasin, James Nankivell and Georgina Virgo (University of Adelaide) for their assistance with fieldwork, and the Geological Survey of South Australia and MinEx CRC for funding the research.

This work is conducted with the appropriate permissions and scientific permits from the relevant stakeholders.

References

Anenburg, M 2020, 'Rare earth mineral diversity controlled by REE pattern shapes', *Mineralogical Magazine*, vol. 84, no. 5, pp. 629-639. doi:10.1180/mgm.2020.70.

Anenburg, M & Williams, MJ 2021, 'Quantifying the Tetrad Effect, Shape Components, and Ce–Eu–Gd Anomalies in Rare Earth Element Patterns', *Mathematical Geosciences*. doi:10.1007/s11004-021-09959-5.

Armistead, SE, Collins, AS, Buckman, S & Atkins, R 2020, 'Age and geochemistry of the Boucaut Volcanics in the Neoproterozoic Adelaide Rift Complex, South Australia', *Australian Journal of Earth Sciences*, pp. 1-10. doi:10.1080/08120099.2021.1840435.

Armit, RJ, Betts, PG, Schaefer, BF, Pankhurst, MJ & Giles, D 2014, 'Provenance of the Early Mesoproterozoic Radium Creek Group in the northern Mount Painter Inlier: Correlating isotopic signatures to inform tectonic reconstructions', *Precambrian Research*, vol. 243, pp. 63-87. doi:10.1016/j.precamres.2013.12.022.

Barovich, KM & Hand, M 2008, 'Tectonic setting and provenance of the Paleoproterozoic Willyama Supergroup, Curnamona Province, Australia: Geochemical and Nd isotopic constraints on contrasting source terrain components', *Precambrian Research*, vol. 166, no. 1, pp. 318-337. doi:10.1016/j.precamres.2007.06.024.

Belousova, EA, Reid, AJ, Griffin, WL & O'Reilly, SY 2009, 'Rejuvenation vs. recycling of Archean crust in the Gawler Craton, South Australia: Evidence from U–Pb and Hf isotopes in detrital zircon', *Lithos*, vol. 113, no. 3-4, pp. 570-582. doi:10.1016/j.lithos.2009.06.028.

Betts, MJ, Paterson, JR, Jacquet, SM, Andrew, AS, Hall, PA, Jago, JB, Jagodzinski, EA, Preiss, WV, Crowley, JL, Brougham, T, Mathewson, CP, García-Bellido, DC, Topper, TP, Skovsted, CB & Brock, GA 2018, 'Early Cambrian chronostratigraphy and geochronology of South Australia', *Earth-Science Reviews*, vol. 185, pp. 498-543. doi:10.1016/j.earscirev.2018.06.005.

Black, LP 2007, *SHRIMP U-Pb zircon ages obtained during 2006/07 for NSW Geological Survey Projects*, no. GS2007/298.

Black, LP & Gulson, BL 1978, 'The age of the Mud Tank Carbonatite, Strangways Range, Northern Territory', *BMR Journal of Australian Geology and Geophysics*, vol. 3, pp. 227-232. http://pid.geoscience.gov.au/dataset/ga/80964.

Bobrovskiy, I, Hope, JM, Ivantsov, A, Nettersheim, BJ, Hallmann, C & Brocks, JJ 2018, 'Ancient steroids establish the Ediacaran fossil Dickinsonia as one of the earliest animals', *Science*, vol. 361, no. 6408, p. 1246. doi:10.1126/science.aat7228.

Brennan, DT, Li, Z-X, Rankenburg, K, Evans, N, Link, PK, Nordsvan, AR, Kirkland, CL, Mahoney, JB, Johnson, T & McDonald, BJ 2021, 'Recalibrating Rodinian rifting in the northwestern United States', *Geology*. doi:10.1130/G48435.1.

Brookfield, ME 1993, 'Neoproterozoic Laurentia-Australia fit', *Geology*, vol. 21, no. 8, pp. 683-686. doi:10.1130/0091-7613(1993)021<0683:NLAF>2.3.CO;2.

Brotodewo, A, Wise, TW & Lloyd, JC 2021, *LA-ICP-MS detrital zircon geochronology from the Delamerian Orogen*, Report Book, no. 2021/00015, Geological Survey of South Australia, DfEa Mining, South Australia.

Callen, RA 1990, *Curnamona*, 1:250 000 Geological Series—Explanatory Notes, Department of Mines and Energy, Adelaide, South Australia.

Calver, CR, Crowley, JL, Wingate, MTD, Evans, DAD, Raub, TD & Schmitz, MD 2013, 'Globally synchronous Marinoan deglaciation indicated by U-Pb geochronology of the Cottons Breccia, Tasmania, Australia', *Geology*, vol. 41, no. 10, pp. 1127-1130. doi:10.1130/g34568.1.

Cawood, PA, Wang, W, Zhao, T, Xu, Y, Mulder, JA, Pisarevsky, SA, Zhang, L, Gan, C, He, H, Liu, H, Qi, L, Wang, Y, Yao, J, Zhao, G, Zhou, M-F & Zi, J-W 2020, 'Deconstructing South China and consequences for reconstructing Nuna and Rodinia', *Earth-Science Reviews*, vol. 204, p. 103169. doi:10.1016/j.earscirev.2020.103169.

Cawood, PA, Zhao, G, Yao, J, Wang, W, Xu, Y & Wang, Y 2018, 'Reconstructing South China in Phanerozoic and Precambrian supercontinents', *Earth-Science Reviews*, vol. 186, pp. 173-194. doi:10.1016/j.earscirev.2017.06.001.

Collins, AS, Reddy, SM, Buchan, C & Mruma, A 2004, 'Temporal constraints on Palaeoproterozoic eclogite formation and exhumation (Usagaran Orogen, Tanzania)', *Earth and Planetary Science Letters*, vol. 224, no. 1, pp. 175-192. doi:10.1016/j.epsl.2004.04.027.

Cooper, PF & Tuckwell, KD 1971, 'The upper Precambrian Adelaidean of the Broken Hill area—a new subdivision', *Quarterly Notes - Geological Survey of New South Wales*, vol. 3, pp. 8-16.

Counts, JW 2017, *The Adelaide Rift Complex in the Flinders Ranges: geologic history, past investigations and relevant analogues*, Report Book, no. 2017/00016, Geological Survey of South Australia, Department of Premier and Cabinet, Adelaide, South Australia, <https://sarigbasis.pir.sa.gov.au/WebtopEw/ws/samref/sarig1/wcir/Record?r=0&m=1&w=catno=2039731>.

Counts, JW & Amos, KJ 2016, 'Sedimentology, depositional environments and significance of an Ediacaran salt-withdrawal minibasin, Billy Springs Formation, Flinders Ranges, South Australia', *Sedimentology*, vol. 63, no. 5, pp. 1084-1123. doi:10.1111/sed.12250.

Counts, JW, Dalgarno, CR, Amos, KJ & Hasiotis, ST 2019, 'Lateral Facies Variability Along the Margin of an Outcropping Salt-Withdrawal Minibasin, South Australia', *Journal of Sedimentary Research*, vol. 89, no. 1, pp. 28-45. doi:10.2110/jsr.2019.2.

Counts, JW, Rarity, F, Ainsworth, RB, Amos, KJ, Lane, T, Morón, S, Trainor, J, Valenti, C & Nanson, R 2016, 'Sedimentological interpretation of an Ediacaran delta: Bonney Sandstone, South Australia', *Australian Journal of Earth Sciences*, vol. 63, no. 3, pp. 257-273. doi:10.1080/08120099.2016.1180322.

Cowley, WM 2020, 'Geological setting of exceptional geological features of the Flinders Ranges', *Australian Journal of Earth Sciences*, pp. 1-23. doi:10.1080/08120099.2020.1748109.

Cox, GM, Isakson, V, Hoffman, PF, Gernon, TM, Schmitz, MD, Shahin, S, Collins, AS, Preiss, WV, Blades, ML, Mitchell, RN & Nordsvan, A 2018, 'South Australian U-Pb zircon (CA-ID-TIMS) age supports globally synchronous Sturtian deglaciation', *Precambrian Research*, vol. 315, pp. 257-263. doi:10.1016/j.precamres.2018.07.007.

Dalziel, IWD 1991, 'Pacific margins of Laurentia and East Antarctica-Australia as a conjugate rift pair: Evidence and implications for an Eocambrian supercontinent', *Geology*, vol. 19, no. 6, pp. 598-601. doi:10.1130/0091-7613(1991)019<0598:PMOLAE>2.3.CO;2.

Danielson, JJ & Gesch, DB 2011, *Global multi-resolution terrain elevation data 2010 (GMTED2010)*, Report, Open-File Report, no. 2011-1073, USG Survey, <http://pubs.er.usgs.gov/publication/ofr20111073>.

Dehler, C, Gehrels, G, Porter, S, Heizler, M, Karlstrom, K, Cox, G, Crossey, L & Timmons, M 2017, 'Synthesis of the 780–740 Ma Chuar, Uinta Mountain, and Pahrump (ChUMP) groups, western USA: Implications for Laurentia-wide cratonic marine basins', *Geological Society of America Bulletin*, vol. 129, no. 5-6, pp. 607-624. doi:10.1130/b31532.1.

Drexel, JF 2008, *Review of the Burra Mine Project, 1980–2008—a progress report*, Report Book, no. 2008/00016, Geological Survey of South Australia, Department of Primary Industries and Resources, South Australia, <https://sarigbasis.pir.sa.gov.au/WebtopEw/ws/samref/sarig1/wci/Record?r=0&m=1&w=catno=2026195>.

Drexel, JF & Preiss, WV (eds) 1995, *The geology of South Australia*, vol. 2, The Phanerozoic, Bulletin, 54, Geological Survey of South Australia, South Australia.

Dröllner, M, Barham, M, Kirkland, CL & Ware, B 2021, 'Every zircon deserves a date: selection bias in detrital geochronology', *Geological Magazine*, vol. 158, no. 6, pp. 1135-1142. doi:10.1017/s0016756821000145.

Eickhoff, KH, Von Der Borch, CC & Grady, AE 1988, 'Proterozoic canyons of the Flinders Ranges (South Australia): submarine canyons or drowned river valleys?', *Sedimentary Geology*, vol. 58, no. 2, pp. 217-235. doi:https://doi.org/10.1016/0037-0738(88)90070-X.

Ernst, RE, Wingate, MTD, Buchan, KL & Li, Z-X 2008, 'Global record of 1600–700Ma Large Igneous Provinces (LIPs): Implications for the reconstruction of the proposed Nuna (Columbia) and Rodinia supercontinents', *Precambrian Research*, vol. 160, no. 1-2, pp. 159-178. doi:10.1016/j.precamres.2007.04.019.

Eyster, A, Weiss, BP, Karlstrom, K & Macdonald, FA 2019, 'Paleomagnetism of the Chuar Group and evaluation of the late Tonian Laurentian apparent polar wander path with implications for the makeup and breakup of Rodinia', *GSA Bulletin*, vol. 132, no. 3-4, pp. 710-738. doi:10.1130/B32012.1.

Fabris, AJ, Constable, SA, Conor, CHH, Woodhouse, A, Hore, SB & Fanning, M 2005, 'Age, origin, emplacement and mineral potential of the Oodla Wirra Volcanics, Nackara Arc, central Flinders Ranges', *MESA Journal*, vol. 37, pp. 44-52. https://sarigbasis.pir.sa.gov.au/WebtopEw/ws/samref/sarig1/wci/Record?r=0&m=1&w=catno=2025119.

Fanning, CM, Ludwig, KR, Forbes, BG & Preiss, WV 1986, 'Single and multiple grain U–Pb zircon analyses for the early Adelaidean Rook Tuff, Willouran Ranges, South Australia', in *Eighth Australian Geological Convention: "Earth Resources in Space and Time"*, Geological Society of Australia, Sydney, New South Wales, pp. 71-72.

Fanning, CM, Reid, AJ & Teale, GS 2007, *A geochronological framework for the Gawler Craton, South Australia*, Bulletin, 55, Geological Survey of South Australia, Adelaide, South Australia.

Fioretti, AM, Black, LP, Foden, J & Visonà, D 2005, 'Grenville-age magmatism at the South Tasman Rise (Australia): A new piercing point for the reconstruction of Rodinia', *Geology*, vol. 33, no. 10, pp. 769-772. doi:10.1130/G21671.1.

Fitzherbert, JA & Downes, PM 2015, 'A concise geological history of the Broken Hill region', *Quarterly Notes - Geological Survey of New South Wales*, vol. 143, no. 2, pp. 29-43.

Fitzsimons, ICW 2000, 'Grenville-age basement provinces in East Antarctica: Evidence for three separate collisional orogens', *Geology*, vol. 28, no. 10, pp. 879-882. doi:10.1130/0091-7613(2000)28<879:GBPIEA>2.0.CO;2.

Flint, RB, Fanning, CM & Rankin, LR 1988, 'The late Proterozoic Kilroo Formation of the Polda Basin', *Quarterly Geological Notes*, vol. 106, pp. 16-23.

Foden, JD, Elburg, MA, Dougherty-Page, J & Burtt, A 2006, 'The timing and duration of the Delamerian orogeny: Correlation with the Ross Orogen and implications for Gondwana assembly', *Journal of Geology*, vol. 114, no. 2, pp. 189-210. doi:10.1086/499570.

Foden, JD, Elburg, MA, Turner, S, Clark, C, Blades, ML, Cox, G, Collins, AS, Wolff, K & George, C 2020, 'Cambro-Ordovician magmatism in the Delamerian orogeny: Implications for tectonic development of the southern Gondwanan margin', *Gondwana Research*. doi:10.1016/j.gr.2019.12.006.

Fraser, GL, McAvaney, S, Neumann, NL, Szpunar, M & Reid, A 2010, 'Discovery of early Mesoarchean crust in the eastern Gawler Craton, South Australia', *Precambrian Research*, vol. 179, no. 1, pp. 1-21. doi:10.1016/j.precamres.2010.02.008.

Fraser, GL & Neumann, NL 2010, *New SHRIMP U-Pb Zircon Ages from the Gawler Craton and Curnamona Province, South Australia, 2008 - 2010*, Record, no. 2010/16, Geoscience Australia, Canberra, <http://pid.geoscience.gov.au/dataset/ga/70348>.

Gain, SEM, Gréau, Y, Henry, H, Belousova, E, Dainis, I, Griffin, WL & O'Reilly, SY 2019, 'Mud Tank Zircon: Long-Term Evaluation of a Reference Material for U-Pb Dating, Hf-Isotope Analysis and Trace Element Analysis', *Geostandards and Geoanalytical Research*, vol. 43, no. 3, pp. 339-354. doi:10.1111/ggr.12265.

Gehling, JG 1983, 'The sedimentology and stratigraphy of the late Precambrian Pound subgroup, Central Flinders Ranges, South Australia', Department of Geology and Mineralogy, Masters Thesis, Masters Degree of Science, University of Adelaide, Adelaide, South Australia, <https://hdl.handle.net/2440/104479>.

Gehling, JG 2000, 'Environmental interpretation and a sequence stratigraphic framework for the terminal Proterozoic Ediacara Member within the Rawnsley Quartzite, South Australia', *Precambrian Research*, vol. 100, no. 1, pp. 65-95. doi:10.1016/S0301-9268(99)00069-8.

Gehling, JG & Droser, ML 2012, 'Ediacaran stratigraphy and the biota of the Adelaide Geosyncline, South Australia', *Episodes*, vol. 35, no. 1, pp. 236-246. doi:10.18814/epiiugs/2012/v35i1/023.

Giddings, JA, Wallace, MW, Haines, PW & Mornane, K 2010, 'Submarine origin for the Neoproterozoic Wonoka canyons, South Australia', *Sedimentary Geology*, vol. 223, no. 1-2, pp. 35-50. doi:10.1016/j.sedgeo.2009.10.001.

Goodge, JW 2020, 'Geological and tectonic evolution of the Transantarctic Mountains, from ancient craton to recent enigma', *Gondwana Research*, vol. 80, pp. 50-122. doi:10.1016/j.gr.2019.11.001.

Goodge, JW, Vervoort, JD, Fanning, CM, Brecke, DM, Farmer, GL, Williams, IS, Myrow, PM & DePaolo, DJ 2008, 'A Positive Test of East Antarctica–Laurentia Juxtaposition Within the Rodinia Supercontinent', *Science*, vol. 321, no. 5886, p. 235. doi:10.1126/science.1159189.

Gostin, VA, Haines, PW, Jenkins, RJF, Compston, W & Williams, IS 1986, 'Impact ejecta horizon within late Precambrian shales, Adelaide geosyncline, South Australia', *Science*, vol. 233, p. 198. https://science.sciencemag.org/content/233/4760/198.long.

Grimes, CB, John, BE, Kelemen, PB, Mazdab, FK, Wooden, JL, Cheadle, MJ, Hanghøj, K & Schwartz, JJ 2007, 'Trace element chemistry of zircons from oceanic crust: A method for distinguishing detrital zircon provenance', *Geology*, vol. 35, no. 7, pp. 643-646. doi:10.1130/G23603A.1.

Grimes, CB, Wooden, JL, Cheadle, MJ & John, BE 2015, '"Fingerprinting" tectono-magmatic provenance using trace elements in igneous zircon', *Contributions to Mineralogy and Petrology*, vol. 170, no. 5, p. 46. doi:10.1007/s00410-015-1199-3.

Haines, PW 1987, 'Carbonate shelf and basin sedimentation, late Proterozoic Wonoka Formation, South Australia', Department of Geology and Geophysics, Doctoral Thesis, Doctor of Philosophy, University of Adelaide, Adelaide, South Australia, <https://hdl.handle.net/2440/21574>.

Hall, JW 2018, 'The thermochronological evolution of the northern Gawler Craton and northern Adelaide Rift Complex', Department of Earth Sciences, Doctoral Thesis, Doctor of Philiosophy, University of Adelaide, Adelaide, South Australia, <https://hdl.handle.net/2440/117807>.

Hoffman, PF 1991, 'Did the Breakout of Laurentia Turn Gondwanaland Inside-Out?', *Science*, vol. 252, no. 5011, pp. 1409-1412. www.jstor.org/stable/2875916.

Horstwood, MSA, Košler, J, Gehrels, GE, Jackson, SE, McLean, NM, Paton, C, Pearson, NJ, Sircombe, KN, Sylvester, P, Vermeesch, P, Bowring, JF, Condon, DJ & Schoene, B 2016, 'Community-Derived Standards for LA-ICP-MS U-(Th-)Pb Geochronology - Uncertainty Propagation, Age Interpretation and Data Reporting', *Geostandards and Geoanalytical Research*, vol. 40, no. 3, pp. 311-332. doi:10.1111/j.1751-908X.2016.00379.x.

Hoskin, PWO & Ireland, TR 2000, 'Rare earth element chemistry of zircon and its use as a provenance indicator', *Geology*, vol. 28, no. 7, pp. 627-630. doi:10.1130/0091-7613(2000)28<627:REECOZ>2.0.CO;2.

Hoskin, PWO & Schaltegger, U 2003, 'The composition of zircon and igneous and metamorphic petrogenesis', *Reviews in Mineralogy and Geochemistry*, vol. 53, no. 1, pp. 27-62. doi:10.2113/0530027.

Howard, HM, Smithies, RH, Kirkland, CL, Kelsey, DE, Aitken, A, Wingate, MTD, Quentin de Gromard, R, Spaggiari, CV & Maier, WD 2015, 'The burning heart — The Proterozoic geology and geological evolution of the west Musgrave Region, central Australia', *Gondwana Research*, vol. 27, no. 1, pp. 64-94. doi:10.1016/j.gr.2014.09.001.

Howchin, W 1904, 'The geology of the Mount Lofty Ranges: Part I', *Transactions of the Royal Society of South Australia*, vol. 28, pp. 253-280.

Hui, B, Dong, Y, Zhang, F, Sun, S & He, S 2021, 'Neoproterozoic active margin in the northwestern Yangtze Block, South China: new clues from detrital zircon U–Pb geochronology and geochemistry of sedimentary rocks from the Hengdan Group', *Geological Magazine*, vol. 158, no. 5, pp. 842-858. doi:10.1017/S0016756820000898.

Ireland, TR, Flöttmann, T, Fanning, CM, Gibson, GM & Preiss, WV 1998, 'Development of the early Paleozoic Pacific margin of Gondwana from detrital-zircon ages across the Delamerian orogen', *Geology*, vol. 26, no. 3, pp. 243-246. doi:10.1130/0091-7613(1998)026<0243:Dotepp>2.3.Co;2.

Jackson, SE, Pearson, NJ, Griffin, WL & Belousova, EA 2004, 'The application of laser ablation-inductively coupled plasma-mass spectrometry to in situ U–Pb zircon geochronology', *Chemical Geology*, vol. 211, no. 1-2, pp. 47-69. doi:10.1016/j.chemgeo.2004.06.017.

Jacobs, J, Elburg, MA, Läufer, A, Kleinhanns, IC, Henjes-Kunst, F, Estrada, S, Ruppel, AS, Damaske, D, Montero, P & Bea, F 2015, 'Two distinct Late Mesoproterozoic/Early Neoproterozoic basement provinces in central/eastern Dronning Maud Land, East Antarctica: The missing link, 15–21°E', *Precambrian Research*, vol. 265, pp. 249-272. doi:10.1016/j.precamres.2015.05.003.

Jacobs, J, Opås, B, Elburg, MA, Läufer, A, Estrada, S, Ksienzyk, AK, Damaske, D & Hofmann, M 2017, 'Cryptic sub-ice geology revealed by a U-Pb zircon study of glacial till in Dronning Maud Land, East Antarctica', *Precambrian Research*, vol. 294, pp. 1-14. doi:10.1016/j.precamres.2017.03.012.

Jago, JB, Gehling, JG, Betts, MJ, Brock, GA, Dalgarno, CR, García-Bellido, DC, Haslett, PG, Jacquet, SM, Kruse, PD, Langsford, NR, Mount, TJ & Paterson, JR 2018, 'The Cambrian System in the Arrowie Basin, Flinders Ranges, South Australia', *Australian Journal of Earth Sciences*, pp. 1-26. doi:10.1080/08120099.2018.1525431.

Jagodzinski, EA & Fricke, CE 2010, *Compilation of new SHRIMP U-Pb geochronological data for the Southern Curnamona Province, South Australia, 2010*, Report Book, no. 2010/00014, Geological Survey of South Australia, Department of Primary Industries and Resources, Adelaide, South Australia.

Jagodzinski, EA & McAvaney, SO 2017, *SHRIMP U-Pb geochronology data for northern Eyre Peninsula, 2014–2016*, Report Book, no. 2016/00001, Geological Survey of South Australia, Adelaide, South Australia, <https://sarigbasis.pir.sa.gov.au/WebtopEw/ws/samref/sarig1/wci/Record?r=0&m=1&w=catno=2039475>.

Jagodzinski, EA, Werner, M, Curtis, S, Fabris, A, Pawley, M & Krapf, C 2020, *SHRIMP Geochronology of the Mt Double area, Southern Gawler Ranges margin*, Report Book, no. 2020/00006, Geological Survey of South Australia, DfEa Mining, South Australia.

Job, AL 2011, 'Evolution of the basal Adelaidean in the northern Flinders Ranges: deposition, provenance and deformation of the Callanna and lower Burra Groups', Department of Geology and Geophysics, Honours Thesis, Bachelor of Science (Honours), University of Adelaide, Adelaide, South Australia, <https://hdl.handle.net/2440/96175>.

Jochum, KP, Weis, U, Stoll, B, Kuzmin, D, Yang, Q, Raczek, I, Jacob, DE, Stracke, A, Birbaum, K, Frick, DA, Günther, D & Enzweiler, J 2011, 'Determination of Reference Values for NIST SRM 610–617 Glasses Following ISO Guidelines', *Geostandards and Geoanalytical Research*, vol. 35, no. 4, pp. 397-429. doi:10.1111/j.1751-908X.2011.00120.x.

Johansson, Å, Bingen, B, Huhma, H, Waight, T, Vestergaard, R, Soesoo, A, Skridlaite, G, Krzeminska, E, Shumlyanskyy, L, Holland, ME, Holm-Denoma, C, Teixeira, W, Faleiros, FM, Ribeiro, BV, Jacobs, J, Wang, C, Thomas, RJ, Macey, PH, Kirkland, CL, Hartnady, MIH, Eglington, BM, Puetz, SJ & Condie, KC 2022, 'A geochronological review of magmatism along the external margin of Columbia and in the Grenville-age orogens forming the core of Rodinia', *Precambrian Research*, p. 106463. doi:10.1016/j.precamres.2021.106463.

Karlstrom, KE & Bowring, SA 1988, 'Early Proterozoic Assembly of Tectonostratigraphic Terranes in Southwestern North America', *The Journal of Geology*, vol. 96, no. 5, pp. 561-576. doi:10.1086/629252.

Karlstrom, KE, Harlan, SS, Williams, ML, McLelland, J, Geissman, JW & Ahäll, K-I 1999, 'Refining Rodinia: geologic evidence for the Australia-western US connection in the Proterozoic', *GSA Today*, vol. 9, no. 10, pp. 1-7.

Keeman, J, Turner, S, Haines, PW, Belousova, E, Ireland, T, Brouwer, P, Foden, J & Wörner, G 2020, 'New UPb, Hf and O isotope constraints on the provenance of sediments from the Adelaide Rift Complex – Documenting the key Neoproterozoic to early Cambrian succession', *Gondwana Research*, vol. 83, pp. 248-278. doi:10.1016/j.gr.2020.02.005.

Kendall, BS, Creaser, RA & Selby, D 2006, 'Re-Os geochronology of postglacial black shales in Australia: Constraints on the timing of “Sturtian” glaciation', *Geology*, vol. 34, no. 9, pp. 729-732. doi:10.1130/g22775.1.

Lan, Z, Li, X-H, Zhu, M, Zhang, Q & Li, Q-L 2015, 'Revisiting the Liantuo Formation in Yangtze Block, South China: SIMS U–Pb zircon age constraints and regional and global significance', *Precambrian Research*, vol. 263, pp. 123-141. doi:10.1016/j.precamres.2015.03.012.

Le Heron, DP 2012, 'The Cryogenian record of glaciation and deglaciation in South Australia', *Sedimentary Geology*, vol. 243-244, pp. 57-69. doi:10.1016/j.sedgeo.2011.09.013.

Le Heron, DP, Cox, GM, Trundley, A & Collins, AS 2011, 'Two Cryogenian glacial successions compared: Aspects of the Sturt and Elatina sediment records of South Australia', *Precambrian Research*, vol. 186, no. 1, pp. 147-168. doi:10.1016/j.precamres.2011.01.014.

Lechte, MA & Wallace, MW 2015, 'Sedimentary and tectonic history of the Holowilena Ironstone, a Neoproterozoic iron formation in South Australia', *Sedimentary Geology*, vol. 329, pp. 211-224. doi:10.1016/j.sedgeo.2015.09.014.

Li, Z-X, Bogdanova, SV, Collins, AS, Davidson, A, De Waele, B, Ernst, RE, Fitzsimons, ICW, Fuck, RA, Gladkochub, DP, Jacobs, J, Karlstrom, KE, Lu, S, Natapov, LM, Pease, V, Pisarevsky, SA, Thrane, K & Vernikovsky, V 2008, 'Assembly, configuration, and break-up history of Rodinia: A synthesis', *Precambrian Research*, vol. 160, no. 1-2, pp. 179-210. doi:10.1016/j.precamres.2007.04.021.

Li, Z-X, Zhang, L & Powell, CM 1995, 'South China in Rodinia: Part of the missing link between Australia–East Antarctica and Laurentia?', *Geology*, vol. 23, no. 5, pp. 407-410. doi:10.1130/0091-7613(1995)023<0407:SCIRPO>2.3.CO;2.

Lindsay, CC 1973, 'Stratigraphy and sedimentology, Mt Saturday area, northern Flinders Ranges, South Australia', Department of Geology, Honours Thesis, Bachelor of Science (Honours), University of Adelaide, Adelaide, South Australia.

Lloyd, JC, Blades, ML, Counts, JW, Collins, AS, Amos, KJ, Wade, BP, Hall, JW, Hore, S, Ball, AL, Shahin, S & Drabsch, M 2020, 'Neoproterozoic geochronology and provenance of the Adelaide Superbasin', *Precambrian Research*, vol. 350, p. 105849. doi:10.1016/j.precamres.2020.105849.

[Dataset] Lloyd, JC, Collins, AS, Blades, ML, Gilbert, SE & Amos, KJ 2022a, 'Burra Group, Yerelina Subgroup, and Pound Subgroup detrital zircon dataset (Lloyd et al.)', *figshare*. doi:10.6084/m9.figshare.19150607.v1.

[Preprint] Lloyd, JC, Collins, AS, Blades, ML, Gilbert, SE & Amos, KJ 2022b, 'Early evolution of the Adelaide Superbasin', *EarthArXiv*. doi:10.31223/X5NH0G.

[Dataset] Lloyd, JC, Collins, AS, Blades, ML, Gilbert, SE & Amos, KJ 2022c, 'LA-ICP-MS detrital zircon standards results', *figshare*. doi:10.6084/m9.figshare.18131432.

[Preprint] Lloyd, JC, Preiss, WV, Collins, AS, Virgo, GM, Blades, ML, Gilbert, SE & Amos, KJ 2022d, 'Detrital zircon record of the Sturtian glaciation: Adelaide Superbasin', *EarthArXiv*.

Lubiniecki, DC, King, RC, Holford, SP, Bunch, MA, Hore, SB & Hill, SM 2020, 'Cenozoic structural evolution of the Mount Lofty Ranges and Flinders Ranges, South Australia, constrained by analysis of deformation bands', *Australian Journal of Earth Sciences*, vol. 67, no. 8, pp. 1097-1115. doi:10.1080/08120099.2019.1695227.

Mackay, WG 2011, 'Structure and sedimentology of the Curdimurka Subgroup, northern Adelaide Fold Belt, South Australia', Doctoral Thesis, Doctor of Philosophy, University of Tasmania, Hobart, Tasmania, <https://eprints.utas.edu.au/12486/>.

MacLennan, SA, Eddy, MP, Merschat, AJ, Mehra, AK, Crockford, PW, Maloof, AC, Southworth, CS & Schoene, B 2020, 'Geologic evidence for an icehouse Earth before the Sturtian global glaciation', *Science Advances*, vol. 6, no. 24, p. eaay6647. doi:10.1126/sciadv.aay6647.

Mancktelow, NS 1979, 'The structure and metamorphism of the southern Adelaide Fold Belt', Department of Geology and Mineralogy, Doctoral Thesis, Doctor of Philosophy, University of Adelaide, Adelaide, South Australia, <https://hdl.handle.net/2440/21024>.

Matenco, LC & Haq, BU 2020, 'Multi-scale depositional successions in tectonic settings', *Earth-Science Reviews*, vol. 200. doi:10.1016/j.earscirev.2019.102991.

Mawson, D 1947, 'The Adelaide Series as developed along the western margin of the Flinders Ranges', *Transactions of the Royal Society of South Australia*, vol. 71, pp. 259-280.

Mawson, D & Sprigg, RC 1950, 'Subdivision of the Adelaide System', *Australian Journal of Science*, vol. 13, no. 3, pp. 69-72.

McAvaney, SO 2012, 'The Cooyerdoo Granite: Paleo- and Mesoarchean basement of the Gawler Craton', *MESA Journal*, vol. 65, pp. 31-40. https://sarigbasis.pir.sa.gov.au/WebtopEw/ws/samref/sarig1/wci/Record?r=0&m=1&w=catno=2035289.

McAvaney, SO, Werner, M, Pawley, MJ, Krapf, CBE & Nicolson, BE 2016, *Geology of the Six Mile Hill 1:75 000 Map Sheet, Mineral Systems Drilling Program Special Map Series*, Report Book, no. 2016/00014, Geological Survey of South Australia, Department of State Development, Adelaide, South Australia.

Meaney, KJ 2012, 'The geochronology and structural evolution of the Warren Inlier and Springfield Sequence, Mt. Lofty Ranges: Implications for Proterozoic paleogeographic reconstructions', School of Earth and Environmental Sciences, Honours Thesis, Bachelor of Science (Honours), University of Adelaide, Adelaide, South Australia, <https://hdl.handle.net/2440/95177>.

Meaney, KJ 2017, 'Proterozoic crustal growth in the southeastern Gawler Craton: the development of the Barossa Complex, and an assessment of the detrital zircon method', Department of Geology and Geophysics, Doctoral Thesis, Doctor of Philosophy, University of Adelaide, Adelaide, South Australia, <https://hdl.handle.net/2440/114255>.

Merdith, AS, Collins, AS, Williams, SE, Pisarevsky, SA, Foden, JD, Archibald, DB, Blades, ML, Alessio, BL, Armistead, SE, Plavsa, D, Clark, C & Müller, RD 2017, 'A full-plate global reconstruction of the Neoproterozoic', *Gondwana Research*, vol. 50, pp. 84-134. doi:10.1016/j.gr.2017.04.001.

Merdith, AS, Williams, SE, Brune, S, Collins, AS & Müller, RD 2019, 'Rift and plate boundary evolution across two supercontinent cycles', *Global and Planetary Change*, vol. 173, pp. 1-14. doi:10.1016/j.gloplacha.2018.11.006.

Merdith, AS, Williams, SE, Collins, AS, Tetley, MG, Mulder, JA, Blades, ML, Young, A, Armistead, SE, Cannon, J, Zahirovic, S & Müller, RD 2021, 'Extending full-plate tectonic models into deep time: Linking the Neoproterozoic and the Phanerozoic', *Earth-Science Reviews*, vol. 214. doi:10.1016/j.earscirev.2020.103477.

Moores, EM 1991, 'Southwest U.S.-East Antarctic (SWEAT) connection: A hypothesis', *Geology*, vol. 19, no. 5, pp. 425-428. doi:10.1130/0091-7613(1991)019<0425:SUSEAS>2.3.CO;2.

Morrissey, LJ, Barovich, KM, Hand, M, Howard, KE & Payne, JL 2019, 'Magmatism and metamorphism at ca. 1.45 Ga in the northern Gawler Craton: The Australian record of rifting within Nuna (Columbia)', *Geoscience Frontiers*, vol. 10, no. 1, pp. 175-194. doi:10.1016/j.gsf.2018.07.006.

Mount, TJ 1976, 'Diapirs and diapirism in the Adelaide 'Geosyncline', South Australia', Department of Geology and Geophysics, PhD Thesis, Doctor of Philosophy, University of Adelaide, Adelaide, South Australia, <https://hdl.handle.net/2440/69802>.

Mulder, JA, Berry, RF, Halpin, JA, Meffre, S & Everard, JL 2018a, 'Depositional age and correlation of the Oonah Formation: refining the timing of Neoproterozoic basin formation in Tasmania', *Australian Journal of Earth Sciences*, vol. 65, no. 3, pp. 391-407. doi:10.1080/08120099.2018.1426629.

Mulder, JA, Everard, JL, Cumming, G, Meffre, S, Bottrill, RS, Merdith, AS, Halpin, JA, McNeill, AW & Cawood, PA 2020, 'Neoproterozoic opening of the Pacific Ocean recorded by multi-stage rifting in Tasmania, Australia', *Earth-Science Reviews*, vol. 201, p. 103041. doi:10.1016/j.earscirev.2019.103041.

Mulder, JA, Karlstrom, KE, Halpin, JA, Merdith, AS, Spencer, CJ, Berry, RF & McDonald, B 2018b, 'Rodinian devil in disguise: Correlation of 1.25–1.10 Ga strata between Tasmania and Grand Canyon', *Geology*, vol. 46, no. 11, pp. 991-994. doi:10.1130/G45225.1.

Murrell, B 1977, 'Stratigraphy and tectonics across the Torrens hinge zone between Andamooka and Marree, South Australia', Department of Geology, Doctoral Thesis, Doctor of Philosophy, University of Adelaide, Adelaide, South Australia, <https://hdl.handle.net/2440/21084>.

Norris, A & Danyushevsky, L 2018, 'Towards Estimating the Complete Uncertainty Budget of Quantified Results Measured by LA-ICP-MS', paper presented at Goldschmidt, Boston.

O'Neill, HSC 2016, 'The Smoothness and Shapes of Chondrite-normalized Rare Earth Element Patterns in Basalts', *Journal of Petrology*, vol. 57, no. 8, pp. 1463-1508. doi:10.1093/petrology/egw047.

Page, RW, Stevens, BPJ & Gibson, GM 2005, 'Geochronology of the Sequence Hosting the Broken Hill Pb-Zn-Ag Orebody, Australia', *Economic Geology*, vol. 100, no. 4, pp. 633-661. doi:10.2113/gsecongeo.100.4.633.

Park, Y, Swanson-Hysell, NL, Xian, H, Zhang, S, Condon, DJ, Fu, H & Macdonald, FA 2021, 'A Consistently High-Latitude South China From 820 to 780 Ma: Implications for Exclusion From Rodinia and the Feasibility of Large-Scale True Polar Wander', *Journal of Geophysical Research: Solid Earth*, vol. 126, no. 6. doi:10.1029/2020jb021541.

Preiss, WV 1987, *Adelaide Geosyncline–late Proterozoic stratigraphy, sedimentation, palaeontology and tectonics*, Bulletin, 53, Geological Survey of South Australia, Adelaide, South Australia.

Preiss, WV 1993, 'Neoproterozoic', in JF Drexel, WV Preiss & AJ Parker (eds), *The geology of South Australia*, vol. 1 The Precambrian, Geological Survey of South Australia, South Australia, pp. 171-204.

Preiss, WV 1997, 'Revision of lithostratigraphy and structure, and evidence of volcanism in Lower Burra Group type sections, Carey Gully-Basket Range Area, Mount Lofty Ranges', *MESA Journal*, vol. 7, pp. 37-46. https://sarigbasis.pir.sa.gov.au/WebtopEw/ws/samref/sarig1/wci/Record?r=0&m=1&w=catno=2020561.

Preiss, WV 1999, *Parachilna*, 1:250 000 Geological Series—Explanatory Notes, Primary Industries and Resources South Australia, Adelaide, South Australia.

Preiss, WV 2000, 'The Adelaide Geosyncline of South Australia and its significance in Neoproterozoic continental reconstruction', *Precambrian Research*, vol. 100, no. 1-3, pp. 21-63. doi:10.1016/S0301-9268(99)00068-6.

Preiss, WV, Alexander, EM, Cowley, WM & Schwarz, MP 2002, 'Towards defining South Australia's geological provinces and sedimentary basins', *MESA Journal*, vol. 27, pp. 39-52. https://sarigbasis.pir.sa.gov.au/WebtopEw/ws/samref/sarig1/wci/Record?r=0&m=1&w=catno=2022981.

Preiss, WV & Cowley, WM 1999, 'Genetic stratigraphy and revised lithostratigraphic classification of the Burra Group in the Adelaide Geosyncline', *MESA Journal*, vol. 14, pp. 30-40. https://sarigbasis.pir.sa.gov.au/WebtopEw/ws/samref/sarig1/wcir/Record?r=0&m=1&w=catno=2025015.

Preiss, WV, Drexel, JF & Reid, AJ 2009, 'Definition and age of the Kooringa Member of the Skillogalee Dolomite: host for Neoproterozoic (c. 790 Ma) porphyry related copper mineralisation at Burra', *MESA Journal*, vol. 55, pp. 19-33. https://sarigbasis.pir.sa.gov.au/WebtopEw/ws/samref/sarig1/wci/Record?r=0&m=1&w=catno=2028895.

Preiss, WV, Dyson, IA, Reid, PW & Cowley, WM 1998, 'Revision of lithostratigraphic classification of the Umberatana Group', *MESA Journal*, vol. 9, pp. 36-42. https://sarigbasis.pir.sa.gov.au/WebtopEw/ws/samref/sarig1/wcir/Record?r=0&m=1&w=catno=2025009.

Preiss, WV, Fanning, CM, Szpunar, MA & Burtt, AC 2008, 'Age and tectonic significance of the Mount Crawford Granite Gneiss and a related intrusive in the Oakbank Inlier, Mount Lofty Ranges, South Australia', *MESA Journal*, vol. 49, pp. 38-49. https://sarigbasis.pir.sa.gov.au/WebtopEw/ws/samref/sarig1/wci/Record?r=0&m=1&w=catno=2026080.

Reid, AJ & Hand, M 2012, 'Mesoarchean to Mesoproterozoic evolution of the southern Gawler Craton, South Australia', *Episodes*, vol. 35, no. 1, pp. 216-225. doi:10.18814/epiiugs/2012/v35i1/021.

Reid, AJ & Jagodzinski, EA (eds) 2011, *PACE Geochronology: Results of collaborative geochronology projects 2009-2010*, Report Book, 2011/00003, Geological Survey of South Australia, Adelaide, South Australia.

Reid, AJ, Jagodzinski, EA, Fraser, GL & Pawley, MJ 2014, 'SHRIMP U–Pb zircon age constraints on the tectonics of the Neoarchean to early Paleoproterozoic transition within the Mulgathing Complex, Gawler Craton, South Australia', *Precambrian Research*, vol. 250, pp. 27-49. doi:10.1016/j.precamres.2014.05.013.

Reid, AJ, Pawley, MJ, Wade, CE, Jagodzinski, EA, Dutch, RA & Armstrong, R 2019, 'Resolving tectonic settings of ancient magmatic suites using structural, geochemical and isotopic constraints: the example of the St Peter Suite, southern Australia', *Australian Journal of Earth Sciences*, vol. 67, no. 1, pp. 31-58. doi:10.1080/08120099.2019.1632224.

Reid, AJ & Payne, JL 2017, 'Magmatic zircon Lu–Hf isotopic record of juvenile addition and crustal reworking in the Gawler Craton, Australia', *Lithos*, vol. 292-293, pp. 294-306. doi:10.1016/j.lithos.2017.08.010.

Retallack, GJ, Marconato, A, Osterhout, JT, Watts, KE & Bindeman, IN 2014, 'Revised Wonoka isotopic anomaly in South Australia and Late Ediacaran mass extinction', *Journal of the Geological Society*, vol. 171, no. 5, p. 709. doi:10.1144/jgs2014-016.

Rooney, AD, Strauss, JV, Brandon, AD & Macdonald, FA 2015, 'A Cryogenian chronology: Two long-lasting synchronous Neoproterozoic glaciations', *Geology*, vol. 43, no. 5, pp. 459-462. doi:10.1130/G36511.1.

Rose, CV, Maloof, AC, Schoene, B, Ewing, RC, Linnemann, U, Hofmann, M & Cottle, JM 2013, 'PAUL F. HOFFMAN SERIES The End-Cryogenian Glaciation of South Australia', *Geoscience Canada*, vol. 40, no. 4, pp. 256-293. doi:10.12789/geocanj.2013.40.019.

Rowan, MG, Hearon Iv, TE, Kernen, RA, Giles, KA, Gannaway-Dalton, CE, Williams, NJ, Fiduk, JC, Lawton, TF, Hannah, PT & Fischer, MP 2019, 'A review of allochthonous salt tectonics in the Flinders and Willouran ranges, South Australia', *Australian Journal of Earth Sciences*, vol. 67, no. 6, pp. 787-813. doi:10.1080/08120099.2018.1553063.

Rubatto, D 2002, 'Zircon trace element geochemistry: partitioning with garnet and the link between U–Pb ages and metamorphism', *Chemical Geology*, vol. 184, no. 1, pp. 123-138. doi:10.1016/S0009-2541(01)00355-2.

Shahin, S 2016, 'Structural analysis and facies distribution of Cryogenian glacial rocks and regional structures in the Willouran Ranges, SA', Department of Earth Sciences, Honours Thesis, Bachelor of Science (Honours), University of Adelaide, Adelaide, South Australia, <https://hdl.handle.net/2440/121230>.

Shannon, RD 1976, 'Revised effective ionic radii and systematic studies of interatomic distances in halides and chalcogenides', *Acta Crystallographica Section A*, vol. 32, no. 5, pp. 751-767. doi:10.1107/S0567739476001551.

Sheard, MJ 2012, *MARREE*, 1:250 000 Series - Explanatory Notes., no. RB2012/00014, Geological Survey of South Australia, I Department for Manufacturing, Trade, Resources and Energy, Adelaide, South Australia.

Sheibner, E & Basden, H (eds) 1998, *Geology of New South Wales - Synthesis*, vol. 13(2), Geology Memoir, Department of Mineral Resources, Sydney, New South Wales.

Shu, L, Yao, J, Wang, B, Faure, M, Charvet, J & Chen, Y 2021, 'Neoproterozoic plate tectonic process and Phanerozoic geodynamic evolution of the South China Block', *Earth-Science Reviews*, vol. 216. doi:10.1016/j.earscirev.2021.103596.

Sláma, J & Košler, J 2012, 'Effects of sampling and mineral separation on accuracy of detrital zircon studies', *Geochemistry Geophysics Geosystems*, vol. 13, no. 5. doi:10.1029/2012gc004106.

Sláma, J, Košler, J, Condon, DJ, Crowley, JL, Gerdes, A, Hanchar, JM, Horstwood, MSA, Morris, GA, Nasdala, L, Norberg, N, Schaltegger, U, Schoene, B, Tubrett, MN & Whitehouse, MJ 2008, 'Plešovice zircon — A new natural reference material for U–Pb and Hf isotopic microanalysis', *Chemical Geology*, vol. 249, no. 1, pp. 1-35. doi:10.1016/j.chemgeo.2007.11.005.

Smithies, RH, Howard, HM, Evins, PM, Kirkland, CL, Bodorkos, S & Wingate, MTD 2008, *The west Musgrave Complex - new geological insights from recent mapping, geochronology, and geochemical studies*, Record, no. 2008/19, Geological Survey of Western Australia, <http://dmpbookshop.eruditetechnologies.com.au/product/the-west-musgrave-complex-new-geological-insights-from-recent-mapping-geochronology-and-geochemical-studies.do>.

Smithies, RH, Howard, HM, Evins, PM, Kirkland, CL, Kelsey, DE, Hand, M, Wingate, MTD, Collins, AS & Belousova, EA 2011, 'High-Temperature Granite Magmatism, Crust–Mantle Interaction and the Mesoproterozoic Intracontinental Evolution of the Musgrave Province, Central Australia', *Journal of Petrology*, vol. 52, no. 5, pp. 931-958. doi:10.1093/petrology/egr010.

Smits, RG, Collins, WJ, Hand, M, Dutch, R & Payne, J 2014, 'A Proterozoic Wilson cycle identified by Hf isotopes in central Australia: Implications for the assembly of Proterozoic Australia and Rodinia', *Geology*, vol. 42, no. 3, pp. 231-234. doi:10.1130/g35112.1.

Spaggiari, CV, Kirkland, CL, Smithies, RH, Wingate, MTD & Belousova, E 2015, 'Transformation of an Archean craton margin during Proterozoic basin formation and magmatism: The Albany–Fraser Orogen, Western Australia', *Precambrian Research*, vol. 266, pp. 440-466. doi:10.1016/j.precamres.2015.05.036.

Sprigg, RC 1952, 'Sedimentation in the Adelaide Geosyncline and the formation of the continental terrace', in MF Glaessner & RC Sprigg (eds), *Sir Douglas Mawson Anniversary Volume*, The University of Adelaide, South Australia, pp. 153-159.

Squire, RJ, Campbell, IH, Allen, CM & Wilson, CJL 2006, 'Did the Transgondwanan Supermountain trigger the explosive radiation of animals on Earth?', *Earth and Planetary Science Letters*, vol. 250, no. 1, pp. 116-133. doi:10.1016/j.epsl.2006.07.032.

Stüeken, EE, Buick, R & Lyons, TW 2019, 'Revisiting the depositional environment of the Neoproterozoic Callanna Group, South Australia', *Precambrian Research*, vol. 334, p. 105474. doi:10.1016/j.precamres.2019.105474.

Swain, G, Woodhouse, A, Hand, M, Barovich, K, Schwarz, M & Fanning, CM 2005, 'Provenance and tectonic development of the late Archaean Gawler Craton, Australia; U–Pb zircon, geochemical and Sm–Nd isotopic implications', *Precambrian Research*, vol. 141, no. 3, pp. 106-136. doi:10.1016/j.precamres.2005.08.004.

Tonkin, DG & Wallace, C 2021, 'Stratigraphy, diagenesis and copper sulfide mineralisation in the Whyalla Sandstone, Stuart Shelf, and implications for stratabound mineral exploration', *MESA Journal*, vol. 94, no. 1, pp. 23-40.

Toteff, S 1977, 'The Geology of the Adelaidean-Kanmantoo Group Sequences in the Eastern Mount Lofty Ranges', Department of Geology and Mineralogy, Doctoral Thesis, Doctor of Philosophy, University of Adelaide, Adelaide, <https://hdl.handle.net/2440/37991>.

Turnbull, RE, Schwartz, JJ, Fiorentini, ML, Jongens, R, Evans, NJ, Ludwig, T, McDonald, BJ & Klepeis, KA 2021, 'A hidden Rodinian lithospheric keel beneath Zealandia, Earth's newly recognized continent', *Geology*, vol. 49, no. 8, pp. 1009-1014. doi:10.1130/g48711.1.

Uppil, RK 1980, 'Sedimentology of the late Precambrian Mundallio Subgroup : a clastic-carbonate (Dolomite, Magnesite) sequence in the Mt. Lofty and Flinders Ranges, South Australia', Department of Geology and Mineralogy, Doctoral Thesis, Doctor of Philosophy, University of Adelaide, Adelaide, South Australia, <https://hdl.handle.net/2440/37784>.

Urlwin, B 1992, 'Carbon isotope stratigraphy of the Late Proterozoic Wonoka Formation of the Adelaide Fold Belt: diagenetic assessment and interpretation of isotopic signature and correlations with previously measured isotopic curves', Department of Geology and Geophysics, Honours Thesis, Bachelor of Science (Honours), University of Adelaide, Adelaide, South Australia, <https://hdl.handle.net/2440/105305>.

van der Wolff, EJ 2020, 'Detrital Provenance and Geochronology of the Burra, Umberatana and Wilpena Groups in the Mount Lofty Ranges', Department of Earth Sciences, Honours Thesis, Bachelor of Science (Honours), University of Adelaide, Adelaide, South Australia.

Verdel, C, Campbell, MJ & Allen, CM 2021, 'Detrital zircon petrochronology of central Australia, and implications for the secular record of zircon trace element composition', *Geosphere*. doi:10.1130/ges02300.1.

Vermeesch, P 2018, 'IsoplotR: a free and open toolbox for geochronology', *Geoscience Frontiers*, vol. 9, no. 5. doi:10.1016/j.gsf.2018.04.001.

Vermeesch, P, Resentini, A & Garzanti, E 2016, 'An R package for statistical provenance analysis', *Sedimentary Geology*, vol. 336, pp. 14-25. doi:10.1016/j.sedgeo.2016.01.009.

Virgo, GM, Collins, AS, Amos, KJ, Farkaš, J, Blades, ML & Subarkah, D 2021, 'Descending into the “snowball”: High resolution sedimentological and geochemical analysis across the Tonian to Cryogenian boundary in South Australia', *Precambrian Research*, vol. 367. doi:10.1016/j.precamres.2021.106449.

Wade, BP, Kelsey, DE, Hand, M & Barovich, KM 2008, 'The Musgrave Province: Stitching north, west and south Australia', *Precambrian Research*, vol. 166, no. 1, pp. 370-386. doi:10.1016/j.precamres.2007.05.007.

Wade, CE 2011, 'Definition of the Mesoproterozoic Ninnerie Supersuite, Curnamona Province, South Australia', *MESA Journal*, vol. 62, pp. 25-42.

Wen, B, Evans, DAD & Li, Y-X 2017, 'Neoproterozoic paleogeography of the Tarim Block: An extended or alternative "missing-link" model for Rodinia?', *Earth and Planetary Science Letters*, vol. 458, pp. 92-106. doi:10.1016/j.epsl.2016.10.030.

Wen, B, Evans, DAD, Wang, C, Li, Y-X & Jing, X 2018, 'A positive test for the Greater Tarim Block at the heart of Rodinia: Mega-dextral suturing of supercontinent assembly', *Geology*, vol. 46, no. 8, pp. 687-690. doi:10.1130/G40254.1.

Wiedenbeck, M, Allé, P, Corfu, F, Griffin, WL, Meier, M, Oberli, F, Quadt, AV, Roddick, JC & Spiegel, W 1995, 'Three Natural Zircon Standards for U-Th-Pb, Lu-Hf, Trace Element and REE Analyses', *Geostandards Newsletter*, vol. 19, no. 1, pp. 1-23. doi:10.1111/j.1751-908X.1995.tb00147.x.

Wiedenbeck, M, Hanchar, JM, Peck, WH, Sylvester, P, Valley, J, Whitehouse, M, Kronz, A, Morishita, Y, Nasdala, L, Fiebig, J, Franchi, I, Girard, JP, Greenwood, RC, Hinton, R, Kita, N, Mason, PRD, Norman, M, Ogasawara, M, Piccoli, PM, Rhede, D, Satoh, H, Schulz-Dobrick, B, Skår, O, Spicuzza, MJ, Terada, K, Tindle, A, Togashi, S, Vennemann, T, Xie, Q & Zheng, YF 2004, 'Further Characterisation of the 91500 Zircon Crystal', *Geostandards and Geoanalytical Research*, vol. 28, no. 1, pp. 9-39. doi:10.1111/j.1751-908X.2004.tb01041.x.

Williams, GE, Gostin, VA, McKirdy, DM & Preiss, WV 2008, 'The Elatina glaciation, late Cryogenian (Marinoan Epoch), South Australia: Sedimentary facies and palaeoenvironments', *Precambrian Research*, vol. 163, no. 3, pp. 307-331. doi:10.1016/j.precamres.2007.12.001.

Williams, GE, Gostin, VA, McKirdy, DM, Preiss, WV & Schmidt, PW 2011, 'The Elatina glaciation (late Cryogenian), South Australia', in E Arnaud, GP Halverson & GA Shields-Zhou (eds), *The Geological Record of Neoproterozoic Glaciations*, Geological Society, London, pp. 713-721.

Williams, GE & Schmidt, PW 2018, 'Shuram–Wonoka carbon isotope excursion: Ediacaran revolution in the world ocean's meridional overturning circulation', *Geoscience Frontiers*, vol. 9, no. 2, pp. 391-402. doi:10.1016/j.gsf.2017.11.006.

Williams, GE & Tonkin, DG 1985, 'Periglacial structures and palaeoclimatic significance of a late Precambrian block field in the Cattle Grid copper mine, Mount Gunson, South Australia', *Australian Journal of Earth Sciences*, vol. 32, no. 3, pp. 287-300. doi:10.1080/08120098508729331.

Williams, MA, Kelsey, DE, Hand, M, Raimondo, T, Morrissey, LJ, Tucker, NM & Dutch, RA 2018, 'Further evidence for two metamorphic events in the Mawson Continent', *Antarctic Science*, vol. 30, no. 1, pp. 44-65. doi:10.1017/S0954102017000451.

Williams, MA & Reid, AJ 2021, 'Linking lithostratigraphy to mineral potential for the Archean to earliest Paleoproterozoic Mulgathing Complex, central Gawler Craton', *MESA Journal*, vol. 94, pp. 4-18.

Wingate, MTD, Campbell, IH, Compston, W & Gibson, GM 1998, 'Ion microprobe U–Pb ages for Neoproterozoic basaltic magmatism in south-central Australia and implications for the breakup of Rodinia', *Precambrian Research*, vol. 87, no. 3, pp. 135-159. doi:10.1016/S0301-9268(97)00072-7.

Wingate, MTD & Giddings, JW 2000, 'Age and palaeomagnetism of the Mundine Well dyke swarm, Western Australia: implications for an Australia–Laurentia connection at 755 Ma', *Precambrian Research*, vol. 100, no. 1, pp. 335-357. doi:10.1016/S0301-9268(99)00080-7.

Wingate, MTD, Pisarevsky, SA & Evans, DAD 2002, 'Rodinia connections between Australia and Laurentia: no SWEAT, no AUSWUS?', *Terra Nova*, vol. 14, no. 2, pp. 121-128. doi:10.1046/j.1365-3121.2002.00401.x.

Wu, G, Xiao, Y, Bonin, B, Ma, D, Li, X & Zhu, G 2018, 'Ca. 850 Ma magmatic events in the Tarim Craton: Age, geochemistry and implications for assembly of Rodinia supercontinent', *Precambrian Research*, vol. 305, pp. 489-503. doi:10.1016/j.precamres.2017.10.020.

Wu, G, Yang, S, Liu, W, Nance, RD, Chen, X, Wang, Z & Xiao, Y 2021, 'Switching from advancing to retreating subduction in the Neoproterozoic Tarim Craton, NW China: Implications for Rodinia breakup', *Geoscience Frontiers*, vol. 12, no. 1, pp. 161-171. doi:10.1016/j.gsf.2020.03.013.

Young, T 1995, 'The Bunyeroo Formation and its possible cold-water marine setting', Department of Geology and Geophysics, Honours Thesis, Bachelor of Science (Hons), University of Adelaide, Adelaide, South Australia.

Zhang, F-Q, Dilek, Y, Cheng, X-G, Wu, H-X, Lin, X-B & Chen, H-L 2019, 'Late Neoproterozoic–early Paleozoic seismic structure–stratigraphy of the SW Tarim Block (China), its passive margin evolution and the Tarim–Rodinia breakup', *Precambrian Research*, vol. 334, p. 105456. doi:10.1016/j.precamres.2019.105456.

Zhao, P, He, J, Deng, C, Chen, Y & Mitchell, RN 2021, 'Early Neoproterozoic (870–820 Ma) amalgamation of the Tarim craton (northwestern China) and the final assembly of Rodinia', *Geology*, vol. 49, no. 11, pp. 1277-1282. doi:10.1130/g48837.1.

Zheng, B, Zhu, W, Ge, R, Wu, H, He, J & Lu, Y 2020, 'Proterozoic tectonic evolution of the Tarim Craton: new insights from detrital zircon U-Pb and Lu-Hf isotopes of metasediments in the Kuruktag area', *Precambrian Research*, p. 105788. doi:10.1016/j.precamres.2020.105788.

Zhou, T, Ge, R, Zhu, W & Wu, H 2021, 'Is there a Grenvillian orogen in the southwestern Tarim Craton?', *Precambrian Research*, vol. 354. doi:10.1016/j.precamres.2020.106053.

Zi, J-W, Haines, PW, Wang, X-C, Jourdan, F, Rasmussen, B, Halverson, GP, Sheppard, S & Li, C-F 2019, 'Pyroxene 40Ar/39Ar Dating of Basalt and Applications to Large Igneous Provinces and Precambrian Stratigraphic Correlations', *Journal of Geophysical Research: Solid Earth*, vol. 124, no. 8. doi:10.1029/2019JB017713.